TKK Dissertations 223
Espoo 2010

SPECTRAL IRRADIANCE AND RADIATION TEMPERATURE SCALES

Doctoral Dissertation

Maija Ojanen

Aalto University
School of Science and Technology
Faculty of Electronics, Communications and Automation
Department of Signal Processing and Acoustics
Metrology Research Institute

TKK Dissertations 223
Espoo 2010

SPECTRAL IRRADIANCE AND RADIATION TEMPERATURE SCALES

Doctoral Dissertation

Maija Ojanen

Doctoral dissertation for the degree of Doctor of Science in Technology to be presented with due permission of the Faculty of Electronics, Communications and Automation for public examination and debate in Auditorium S5 at the Aalto University School of Science and Technology (Espoo, Finland) on the 21st of May 2010 at 12 noon.

Aalto University
School of Science and Technology
Faculty of Electronics, Communications and Automation
Department of Signal Processing and Acoustics
Metrology Research Institute

Aalto-yliopisto
Teknillinen korkeakoulu
Elektroniikan, tietoliikenteen ja automaation tiedekunta
Signaalinkäsittelyn ja akustiikan laitos
MIKES – Aalto Mittaustekniikka

Distribution:
Aalto University
School of Science and Technology
Faculty of Electronics, Communications and Automation
Department of Signal Processing and Acoustics
Metrology Research Institute
P.O. Box 13000 (Otakaari 5A)
FI - 00076 Aalto
FINLAND
URL: http://spa.tkk.fi/
URL: http://metrology.tkk.fi/
Tel. +358-9-47001
Fax +358-9-470 22222
E-mail: maija.ojanen@tkk.fi

ISBN 978-952-60-3155-2
ISBN 978-952-60-3156-9 (PDF)
ISSN 1795-2239
ISSN 1795-4584 (PDF)
URL: http://lib.tkk.fi/Diss/2010/isbn9789526031569/

TKK-DISS-2758

Picaset Oy
Helsinki 2010

Aalto University

ABSTRACT OF DOCTORAL DISSERTATION	AALTO UNIVERSITY SCHOOL OF SCIENCE AND TECHNOLOGY P.O. BOX 11000, FI-00076 AALTO http://www.aalto.fi

Author Maija Ojanen

Name of the dissertation
Spectral Irradiance and Radiation Temperature Scales

Manuscript submitted 2.2.2010	Manuscript revised 20.4.2010
Date of the defence 21.5.2010	
☐ Monograph	☒ Article dissertation (summary + original articles)

Faculty	Faculty of Electronics, Communications and Automation
Department	Department of Signal Processing and Acoustics
Field of research	Measurement Science and Technology
Opponent(s)	Dr. Arnold A. Gaertner, National Research Council Canada
Supervisor	Prof. Erkki Ikonen
Instructor	Prof. Petri Kärhä

Abstract

Spectral irradiance and radiation temperature measurements are needed in various applications, from environmental studies to different fields of industry. Scale realizations are needed to serve the calibration needs of these applications.

In this thesis, I present various improvements to the scales of spectral irradiance and radiation temperature. A physical model was developed for tungsten halogen lamps utilized as spectral irradiance sources. The model consists of Planck's radiation law, emissivity of tungsten in polynomial form, and a correction function. The model can interpolate the spectral irradiance values of lamps with an agreement better than 1 % with previous calibrations by MIKES/TKK and NPL (UK) throughout the spectral region 340 nm – 850 nm.

Spectral irradiance scales of MIKES/TKK and NMC (Singapore) were compared using an automated multi-wavelength filter radiometer. The wavelength range of the comparison was 290 nm – 900 nm. The agreement was compared with the results of the previous key comparison. The results indicated that the long-term reproducibility of the spectral irradiance scale of MIKES is excellent in the wavelength range above 400 nm. In the range 290 nm – 400 nm, the reproducibility is within 2.8 %, which is still within the expanded uncertainties of the comparison.

The spectral irradiance scale of NIMT (Thailand) was linked to the CIPM key comparison reference value using MIKES as a link in a bilateral key comparison. I present a method for uncertainty estimation in linking key comparisons.

A detector-based radiation temperature scale was developed at MIKES. Filter radiometers were first compared with a Ag fixed point cell, and then with a linear pyrometer in the temperature range of 1370 K – 1770 K. With help of the filter radiometers, the extrapolation of the pyrometer readings could be studied.

The radiation temperature scales of MIKES and PTB (Germany) were compared in the range 1570 K – 2770 K. Both the International Temperature Scale of 1990 (ITS-90) and thermodynamic temperature scales were compared. The ITS-90 based scales were in agreement. The agreement of the thermodynamic temperature scales was partial: The results for two out of four filter radiometers of MIKES agreed with each other and with those of PTB, whereas the results from the two others showed deviations. Possible reasons for this deviation, such as differences in measurement geometries and possible diffuse transmittance in the interference filters, are postulated and discussed.

Keywords: Filter radiometer, key comparison, radiation temperature, spectral irradiance, tungsten halogen lamp, uncertainty evaluation

ISBN (printed) 978-952-60-3155-2	ISSN (printed) 1795-2239
ISBN (pdf) 978-952-60-3156-9	ISSN (pdf) 1795-4584
Language English	Number of pages 65 p. + appendix 42 p.
Publisher Metrology Research Institute, Aalto University, School of Science and Technology	
Print distribution Metrology Research Institute, Aalto University, School of Science and Technology	

☒ The dissertation can be read at http://lib.tkk.fi/Diss/2010/isbn9789526031569/

VÄITÖSKIRJAN TIIVISTELMÄ	AALTO-YLIOPISTO TEKNILLINEN KORKEAKOULU PL 11000, 00076 AALTO http://www.aalto.fi
Tekijä Maija Ojanen	
Väitöskirjan nimi Spektrisen irradianssin ja säteilylämpötilan mitta-asteikot	
Käsikirjoituksen päivämäärä 2.2.2010	Korjatun käsikirjoituksen päivämäärä 20.4.2010
Väitöstilaisuuden ajankohta 21.5.2010	
☐ Monografia	☒ Yhdistelmäväitöskirja (yhteenveto + erillisartikkelit)
Tiedekunta Elektroniikan, tietoliikenteen ja automaation tiedekunta Laitos Signaalinkäsittelyn ja akustiikan laitos Tutkimusala Mittaustekniikka Vastaväittäjä(t) Tri Arnold A. Gaertner, National Research Council Canada Työn valvoja Prof. Erkki Ikonen Työn ohjaaja Prof. Petri Kärhä	

Tiivistelmä

Spektrisen irradianssin ja säteilylämpötilan mittauksia käytetään lukuisissa sovelluksissa, kuten ympäristötutkimuksessa ja useilla teollisuuden aloilla. Näiden sovellusten kalibrointitarpeita varten tarvitaan mitta-asteikkojen toteutuksia.

Tässä työssä esitetään useita parannuksia spektrisen irradianssin ja säteilylämpötilan mitta-asteikkoihin. Työssä on kehitetty fysikaalinen malli spektrisen irradianssin lähteenä käytettävälle volframihalogeenilampulle. Malli koostuu Planckin säteilylaista, volframin emissiivisyydestä polynomimuodossa, sekä korjaustekijästä. Mallin avulla voidaan interpoloida lampun spektrinen irradianssi aallonpituusalueella 340 nm – 850 nm 1 % yhtäpitävyydellä MIKES/TKK:n ja NPL:n (UK) aiempien kalibrointien kanssa.

MIKES/TKK:n ja NMC:n (Singapore) spektrisen irradianssin mitta-asteikkoja verrattiin useammalla aallonpituudella toimivan automatisoidun suodatinradiometrin avulla. Vertailun aallonpituusalue oli 290 nm – 900 nm. Yhtäpitävyyttä verrattiin aiemman avainvertailun tuloksiin. Vertailu osoitti MIKES/TKK:n spektrisen irradianssin mitta-asteikon pitkän ajan toistuvuuden olevan erittäin hyvä aallonpituuden 400 nm yläpuolella. Alueella 290 nm – 400 nm pitkän ajan toistuvuus oli heikoimmillaan 2,8 %, mikä on kuitenkin vertailun laajennetun epävarmuuden puitteissa.

NIMT:n (Thaimaa) spektrisen irradianssin mitta-asteikko linkitettiin CIPM:n avainvertailun referenssiarvoon käyttäen MIKESiä linkkinä kahdenvälisessä avainvertailussa. Työssä esitetään menetelmä epävarmuuksien arviointiin avainvertailujen linkityksessä.

MIKESissä kehitettiin detektoripohjainen säteilylämpötila-asteikko. Suodatinradiometrien toiminta varmennettiin hopeakiintopisteessä. Tämän jälkeen suodatinradiometrejä verrattiin lineaaripyrometriin lämpötila-alueella 1370 K – 1770 K. Suodatinradiometrimittausten avulla voitiin tutkia pyrometrin mittausarvojen ekstrapolointia.

MIKESin ja and PTB:n (Saksa) säteilylämpötila-asteikkoja verrattiin lämpötila-alueella 1570 K – 2770 K. Vertailu sisälsi sekä kansainvälisen lämpötila-asteikon (ITS-90) mukaisen että termodynaamisen lämpötila-asteikon vertailun. ITS-90 – pohjaiset asteikot olivat yhtäpitävät. Termodynaamisten asteikkojen yhtäpitävyys oli osittainen. Kaksi neljästä MIKESin suodatinradiometristä oli yhtäpitävät sekä keskenään että PTB:n tulosten kanssa, mutta kahden suodatinradiometrin tuloksissa havaittiin poikkeamia. Työssä esitellään ja pohditaan poikkeamien mahdollisia syitä, kuten eroja mittausgeometrioissa sekä interferenssisuodatinten hajaläpäisyä.

Asiasanat Epävarmuusarvio, spektrinen irradianssi, suodatinradiometri, säteilylämpötila, vertailumittaus, volframihalogeenilamppu	
ISBN (painettu) 978-952-60-3155-2	ISSN (painettu) 1795-2239
ISBN (pdf) 978-952-60-3156-9	ISSN (pdf) 1795-4584
Kieli Englanti	Sivumäärä 65 s. + liitteet 42 s.
Julkaisija MIKES – Aalto Mittaustekniikka, Aalto-yliopisto, Teknillinen korkeakoulu	
Painetun väitöskirjan jakelu MIKES – Aalto Mittaustekniikka, Aalto-yliopisto, Teknillinen korkeakoulu	
☒ Luettavissa verkossa osoitteessa http://lib.tkk.fi/Diss/2010/isbn9789526031569/	

Preface

The research work for this thesis has been carried out at the Metrology Research Institute (MRI) of the Aalto University, School of Science and Technology during years 2006-2009. The research has been carried out in collaboration with the Centre for Metrology and Accreditation (MIKES), Physikalisch-Technische Bundesanstalt (PTB), National Metrology Centre (NMC) and National Institute of Metrology, Thailand (NIMT).

I would like to thank my supervisor, Professor Erkki Ikonen, for giving me the opportunity to work with this research project, and for the guidance during this work. I would also like to express my gratitude to my instructor, Professor Petri Kärhä, for the guidance during the research and writing processes.

I would like to thank Dr. Martti Heinonen and Dr. Thua Weckström from MIKES for giving me the opportunity to use the radiation temperature measurement facilities of MIKES and for the guidance in practical measurements.

I am grateful to all my co-authors and colleagues at the MRI. Special thanks to Dr. Silja Holopainen for all the help, fun and fruitful discussions.

Part of the research work was carried out at PTB, Berlin. I would like to thank PD Dr. Jürgen Hartmann and Dr. Klaus Anhalt for giving me this opportunity. The practical assistance by Mr. Stephan Schiller is acknowledged.

I wish to thank Dr. Rojana Leecharoen (NIMT), Dr. Yuanjie Liu (NMC) and Dr. Gan Xu (NMC) for collaboration in spectral irradiance comparisons.

The preliminary examiners, Dr. Emma Woolliams and Professor Folke Stenman, are thanked for their efforts.

I wish to thank my high school mathematics and physic teachers, Sakari Salonen and Sirkku Haapala, for encouragement towards scientific studies.

The financial support by Finnish Foundation for Technology Promotion (Tekniikan Edistämissäätio), Emil Aaltonen foundation, Jenny and Antti Wihuri Foundation, and the Graduate School of Electrical and Communications Engineering is acknowledged.

Finally I would like to thank my parents, my sister Tiina, and my fiancé Jarkko for their love and support.

Espoo, April 2010

Maija Ojanen

Contents

List of Publications

This thesis consists of an overview and the following selection of the author's publications.

I M. Ojanen, P. Kärhä and E. Ikonen: "Spectral irradiance model for tungsten halogen lamps in 340-850 nm wavelength range," *Applied Optics* **49**, 880-886 (2010).

II Y. J. Liu, G. Xu, M. Ojanen and E. Ikonen, "Spectral irradiance comparison using a multi-wavelength filter radiometer," *Metrologia* **46**, S181-185 (2009).

III M. Ojanen, M. Shpak, P. Kärhä, R. Leecharoen and E. Ikonen, "Uncertainty evaluation for linking a bilateral key comparison with the corresponding CIPM key comparison," *Metrologia* **46**, 397-403 (2009).

IV M. Ojanen, V. Ahtee, M. Noorma, T. Weckström, P. Kärhä and E. Ikonen, "Filter radiometers as a tool for quality assurance of temperature measurements with linear pyrometers," *International Journal of Thermophysics* **29**, 1084-1093 (2008).

V M. Ojanen, K. Anhalt, J. Hartmann, S. Schiller, T. Weckström, P. Kärhä, M. Heinonen and E. Ikonen, "Comparison of the radiation temperature scales between MIKES and PTB," *Measurement* **43**, 183-189 (2010).

Author's Contribution

All the publications included in this thesis are results of team work.

For Publication I, the author carried out the measurements and analysis of the results, and prepared the manuscript.

For Publication II, the author carried out the measurements at MIKES/TKK and analyzed the results of MIKES/TKK and part of the results of NMC.

For Publication III, the author carried out the measurements at MIKES/TKK, calculated the degrees of equivalence and corresponding uncertainties for NIMT, and prepared the manuscript.

For Publication IV, the author carried out the latest measurements and analyses of 2006, and prepared the manuscript.

For Publication V, the author visited PTB, participated in carrying out the measurements, analyzed the results of MIKES, and prepared the manuscript.

List of Abbreviations

ANSI	American National Standards Institute
BIPM	Bureau International des Poids et Mesures
CCPR	Consultative Committee for Photometry and Radiometry
CCT	Consultative Committee for Thermometry
CIPM	International Committee of Weights and Measures
CODATA	Committee on Data for Science and Technology
DoE	Degree of equivalence
EUV	Extreme ultraviolet
F	Freezing point
FPC	Fixed point cell
FR	Filter radiometer
G	Gas thermometer point
HTBB	High temperature blackbody
IFA-CSIC	Instituto de Física Aplicada – Consejo Superior de Investigaciones Científicas, Spain
ITS-90	International Temperature Scale of 1990
KCRV	Key Comparison Reference Value
KRISS	Korea Research Institute of Standards and Science
LP	Linear pyrometer
M	Melting point
M(C)-C	Metal-(carbon)-carbide
MIKES	Mittatekniikan keskus, Centre for Metrology and Accreditation, Finland
MRA	Mutual Recognition Arrangement
MWFR	Multi-wavelength filter radiometer
NIMT	National Institute of Metrology, Thailand
NIR	Near infrared
NIST	National Institute of Standards and Technology, USA
NMC	National Metrology Centre, Singapore
NMI	National Metrology Institute
NMIJ	National Metrology Institute of Japan
NMi-VSL	Nederlands Meetinstituut – Van Swinden Laboratorium, the Netherlands
NPL	National Physical Laboratory, UK
NRC	National Research Council, Canada
PriTeRa	Primary Temperature Radiator
PRT	Platinum resistance thermometer
PTB	Physikalisch-Technische Bundesanstalt, Germany
PLTS	Provisional Low Temperature Scale
RMO	Regional Metrology Organization
SI	Système international d'unités, International System of Units
T	Triple point
TKK	Helsinki University of Technology
UME	Ulusal Metroloji Enstitüsü, Turkey

UV	Ultraviolet
VNIIOFI	All-Russian Research Institute for Optical and Physical Measurements
V	Vapor pressure point
VTBB	Variable temperature blackbody
WG	Working group

List of Symbols

A	Area
A_{BB}	Area of a blackbody
a	Dimension
α	Index for an NMI
B	Magnetic field
B, $B(T)$	Geometrical coefficient
b	Coefficient
b	Dimension
c	Speed of light in vacuum, 299792458 m/s
c_2	Second radiation constant defined by CODATA, 1.4388×10^{-2} m K
D_i, D_j, D_α	Degree of equivalence
D	Geometrical factor
d	Distance
Δ	Difference
E	Photon energy
E_{kc}	Error component related to key comparison
E_{b}	Error component related to uncorrelated effects between measurements and transfer
E_{r}	Error component related to scale reproducibility
$E(\lambda,T)$	Spectral irradiance as a function of temperature
$E_{\mathrm{c}}(\lambda)$	Calculated spectral irradiance
$E_{\mathrm{m}}(\lambda)$	Measured spectral irradiance
e	Neper constant, 2.71828
ε	Emissivity
$\varepsilon(\lambda)$	Spectral emissivity
$\varepsilon(\lambda,T)$	Spectral emissivity as a function of temperature
$\varepsilon_{\mathrm{W}}(\lambda,T)$	Emissivity of tungsten
$\varepsilon_{\Delta}(\lambda,T)$	Residual correction for emissivity
Φ_E	Photon flux at energy E
h	Planck constant, $6.6260755 \times 10^{-34}$ J s
I	Current
I	Linking invariant
i	Index for an NMI
i_{c}	Calculated photocurrent
i_{cal}	Calibration current
i_{m}	Measured photocurrent
i_{ph}	Photocurrent
j	Index
k	Boltzmann constant, $1.3806505 \times 10^{-23}$ J K^{-1}
k	Coverage factor
κ	Attenuation factor
$L(\lambda,T)$	Spectral radiance

λ	Wavelength
λ_{eff}	Effective wavelength
N	Degree of a polynomial
R	Resistance
$R(\lambda)$	Spectral responsivity
r_{BB}	Radius of a blackbody aperture
r_{FR}	Radius of a filter radiometer aperture
ρ	Reflectance
$S(\lambda)$	Spectral responsivity of a detector
$s(T)$	Thermometer signal
Σ_y	Effective vertical source size
T, T_1, T_2	Thermodynamic temperature
T_{90}	ITS-90 temperature
$\tau(\lambda)$	Spectral transmittance
U	Expanded uncertainty
u	Standard uncertainty
u_{kc}	Standard uncertainty related to key comparison
u_b	Standard uncertainty related to uncorrelated effects between measurements and transfer
u_r	Standard uncertainty related to scale reproducibility
X_{ref}	Key comparison reference value
Ξ	Measured value
ξ	Coefficient related to optical properties
Ψ	Vertical emission angle
W	Electron energy
W	Reference function for temperature calculation
w	Weighting factor

1 Introduction

1.1 Background

The goal of this thesis is to develop and improve methods for performing accurate spectral irradiance and temperature measurements using spectroradiometric methods. Measurements of optical radiation are needed in various fields of science and industry, in atmospheric and solar studies, remote sensing, military applications, and in metal, paper and food industry. The interest may be related with the optical power, or with the radiation temperature. For example, meteorological institutes use spectroradiometers for solar spectral irradiance measurements, especially in the ultraviolet (UV) region. Optical measurements are also used to determine high temperatures through pyrometry – the applications are growing, particularly for the manufacture of novel composite materials used e.g. in aerospace industry.

Many of the technical challenges for both radiation thermometry and spectral irradiance are linked through blackbody radiation and filter radiometry. The connection between the output spectrum and the temperature of a blackbody radiator is established by Planck's radiation law [1]. The output spectrum of a radiation source can be determined from its temperature, if the emissivity of the source is known. Alternatively, the temperature of an object can be determined by measuring its radiation spectrum.

The International Temperature Scale of 1990 (ITS-90) has been defined to approximate the thermodynamic temperature in order to assist the practical temperature measurements and calibrations. The ITS-90 is based on several fixed temperature points and interpolation equations between them. The ITS-90 utilizes Planck's radiation law as an interpolation equation between silver and copper freezing points, 1234.93 K and 1357.77 K, and as an extrapolation equation above the copper freezing point [2]. High-temperature fixed points [3,4,5,6,7,8] provide access to thermodynamic temperatures for the calibration of radiation thermometers. In addition, they will provide a means of confirming filter radiometer measurements, which are also used for spectral irradiance measurements.

Despite the different quantities measured and their corresponding units, the methods and techniques used in spectral irradiance and radiation temperature measurements are quite similar [9]. Development of filter radiometry has benefited both realizing spectral irradiance scales [10,11,12] and measurements of the thermodynamic temperature [13,14,15,16]. Development of high temperature blackbody sources (HTBBs) [17,18] has assisted both spectral irradiance and radiation temperature scale realizations.

Tungsten halogen lamps [19] are often used as affordable and easy-to-operate working standards for spectral irradiance measurements. Due to their compact size, they are often used as transfer standards in intercomparisons. Some research institutes and industrial companies utilize them in order to obtain traceability to the national scales.

National metrology institutes (NMIs) maintain measurement standards traceable to the International System of Units (SI), and offer calibration services. The scales maintained for calibration purposes require quality assurance. Intercomparisons provide a way to check the quality and to study the long-term stability of the scales. Different types of comparisons are carried out: International Committee of Weights and Measures (CIPM) key comparisons [20,21], regional and bilateral key comparisons [22,Publ.III], and informal comparisons [Publ.II,Publ.V]. It has been agreed that only the CIPM key comparison provides a key comparison reference value (KCRV), to which other NMIs can then be linked using regional or bilateral comparisons [Publ.III]. In simplest form of the comparison, the different scales realized for the same quantity may be used to assure the quality of each other within one institute [23,Publ.IV].

1.2 Progress of the work

In order to allow quicker, fit-for-purpose calibrations of tungsten halogen lamps, I have developed a physical model for tungsten halogen lamps [Publ.I]. The model consists of Planck's radiation law, emissivity of tungsten [24] in polynomial form [25], and a correction for the residual emissivity. The model can interpolate the spectral irradiance values of 1-kW tungsten halogen lamps of types FEL[1] and DXW with an agreement better than 1 % throughout the spectral region studied. I also demonstrate determination of the spectral irradiance 1) with knowledge of the color temperature and the illuminance value of the lamp and 2) with knowledge of electrical properties of the lamp [Publ.I].

As part of the international work to ensure consistency of spectral irradiance scales, I have carried out two comparisons and developed a new approach for analyzing linked comparisons. The MIKES/TKK spectral irradiance scale was compared with the scales of National Metrology Centre (NMC, Singapore) [Publ.II] and National Institute of Metrology, Thailand (NIMT) [Publ.III]. The measurement results showed good agreement between the MIKES/TKK and NMC [Publ.II]. The scales were also compared via the recent key comparisons CCPR-K1.a [20] and CCPR-K1.a.1 [26], which gave useful information on the long-term reproducibility of the spectral irradiance scales of the compared NMIs to be used in the following research [Publ.III].

In [Publ.III], the spectral irradiance scale of NIMT was linked to the CIPM KCRV using MIKES as a link. I present a method for uncertainty estimation in linking intercomparisons. The method recommends dividing the uncertainties of the linking NMI into uncertainties due to correlated and uncorrelated effects. With help of the method, the uncertainty due to linking can be realistically estimated and a suitable linking NMI can be selected.

[1] FEL and DXW are codes of the lamps, defined by American National Standards Institute (ANSI).

A detector-based temperature measurement facility was applied for radiation temperature measurements at MIKES [Publ.IV]. Absolutely calibrated filter radiometers were used to assure the quality of the extrapolation of a linear pyrometer in the temperature range of 1370 K to 1800 K.

As with spectral irradiance, comparisons are also important to ensure the stability and accuracy of temperature measurement facilities. I visited Physikalisch-Technische Bundesanstalt (PTB, Germany) and participated in carrying out an intercomparison of the radiation temperature scales of MIKES and PTB. The scales were compared in the range 1570 K – 2770 K. Both thermodynamic temperature measurements and relative temperature measurements based on the ITS-90 were compared. The ITS-90 based scales were in agreement within uncertainties. The agreement was partial in the measurements of the thermodynamic temperature: two out of four MIKES filter radiometers showed agreement with the PTB filter radiometer and the ITS-90 based scales [Publ.V].

This thesis is organized as follows: Chapter 2 gives an overview of spectral irradiance sources and scale realizations. A new model for tungsten halogen lamps used as spectral irradiance sources is presented [Publ.I]. The chapter continues with a description of two intercomparisons in spectral irradiance [Publ.II,Publ.III]. A method for uncertainty estimation in linking intercomparisons is presented using a linking intercomparison between MIKES and NIMT as a practical example [Publ.III]. Chapter 3 begins with a description of the ITS-90 and a discussion on its future trends. Then, radiation temperature measurements at MIKES [Publ.IV] and an intercomparison between MIKES and PTB [Publ.V] are presented. Conclusions of this work are presented in Chapter 4.

1.3 Scientific contribution

This thesis contains the following new scientific results:

1. A new, physical model for tungsten halogen lamps is developed. The model provides the first evidence that a tungsten halogen lamp can be used as an absolute source for spectral irradiance. To our knowledge, such research efforts have not been published earlier.

2. A novel method for estimating uncertainties in linking intercomparisons is presented. The findings are expected to be useful for the preparation of new key comparisons and linking them to regional comparisons.

3. Quality assurance of pyrometer measurements using irradiance mode filter radiometers is demonstrated. Verification of pyrometer measurements is essential for extrapolated temperature measurements above the last ITS-90 fixed point, freezing point of Cu at 1357.77 K.

2 Spectral irradiance

2.1 Standard radiation sources in metrology

The radiation sources in metrology can be divided into primary and secondary sources. The primary sources are based around a physical law and a measurement of a single, unrelated quantity, whereas the secondary sources require calibration with a primary method.

2.1.1 Primary radiation sources

Blackbodies

Planck’s radiation law connects the spectral radiance $L(\lambda,T)$ and the temperature T of a blackbody radiator through

$$L(\lambda,T)=\frac{2hc^2\varepsilon}{\lambda^5\left[\exp\left(\frac{hc}{\lambda kT}\right)-1\right]}, \tag{1}$$

where λ is the wavelength in vacuum, h is the Planck constant, c is the speed of light in vacuum, k is the Boltzmann constant and ε is the emissivity of the radiator cavity. The emissivity of an ideal blackbody radiator is unity. In principle, a correction for the refractive index of air is also required.

Practical blackbody radiators consist of a uniformly heated cavity with an opening, which is small compared to the size of the cavity. The shape of the cavity may be spherical, cylindrical or conical, or the cavity may consist of a conical back wall and cylindrical side walls. A schematic of a spherical cavity is presented in Figure 1.

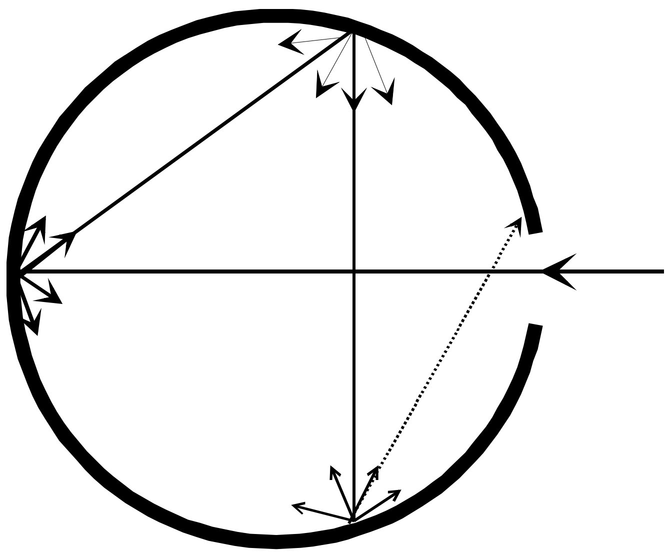

Figure 1. Schematic of a spherical cavity of a blackbody radiator.

If the temperature and the emissivity of the cavity are known, the radiation emitted through the opening can be determined using Eq. (1). The emissivity of a practical blackbody can be close to unity: for standard laboratory sources the emissivity is typically higher than 0.98 [27], and for high-quality blackbodies higher than 0.999 [17,28]. The emissivity can be determined by reflection measurements [28], or by Monte Carlo simulation [28,29]. The wavelength dependence of the emissivity is usually small. It is thus possible to extrapolate the spectral irradiance to other wavelengths using blackbodies.

Blackbody radiators may be used as variable temperature sources, or their temperatures may be stabilized to phase transitions of metals using fixed point cells (FPCs). The FPCs are made of pure metal shielded in a graphite crucible. The purity of the metal should nominally be 99.999% [30]. The metals used in the FPCs include zinc, aluminium, silver, gold and copper, whose freezing point temperatures are defined by the ITS-90 [2]. A schematic of an FPC is presented in Figure 2.

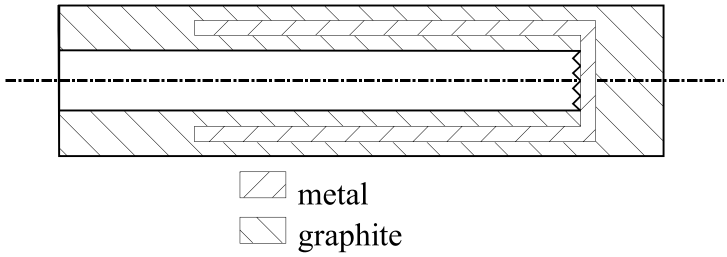

Figure 2. Structure of a fixed point cell.

FPCs are typically operated in resistance heated furnaces. First, the cell is placed into a furnace, whose temperature is set to 5 °C – 10 °C above the melting point of the metal. After melting, the temperature of the metal rises to the set point of the furnace. To obtain the freezing plateau, the temperature of the furnace is set below the freezing point. The temperature of the furnace starts to drop, and the metal undergoes a supercool, i.e. a temperature drop of the liquid metal below its freezing point. This takes place before the molten metal starts to freeze. The supercool for silver and copper is typically less than 0.5 K lower than the freezing point. After the short supercool, the temperature rises back to the freezing point and the freezing plateau is reached. The temperature of the cell stays constant typically for a couple of hours. A gas flow of nitrogen or argon may be channeled to the graphite shielding in order to prevent oxidation of the shielding [30].

Variable-temperature blackbodies (VTBBs) are divided into four categories [18]: high-temperature blackbodies (HTBBs, operating temperature 1800 K – 3200 K), middle-temperature blackbodies (400 K – 1800 K), low-temperature blackbodies (200 K – 400 K) and cryogenic blackbodies (60 K – 200 K). The VTBBs used as spectral irradiance sources are typically HTBBs made of graphite or pyrolytic graphite [17]. The advantage of pyrolytic graphite is that its sublimation rate is lower than for ordinary graphite. The drawback is that it cannot be machined as a radiator with a long cylindrical cavity, and thus the cavities consist of pyrolytic graphite rings [17]. The radiator may be heated by electric current conducted directly through it [17]. To obtain good electrical contacts, the rings may be attached to each other using a spring arrangement, as in a commonly used HTBB model, BB3200pg [17]. The housing of the HTBB is often water-cooled.

HTBBs are used as radiation sources in the wavelength range 200 nm – 3000 nm [18]. In order to obtain reasonable spectral irradiance levels in the UV region, they must be operated at temperatures above 3200 K [18,31]. In this temperature range, absorption of the radiation due to the increased molecular sublimation rate of carbon may occur, even if pyrolytic graphite is used as cavity material [31,32]. To detect these absorptions, the blackbody must be thoroughly characterized before operation, especially in the UV region [32].

The uniformity and stability properties of HTBBs have been studied in [18,33,34,35]. At a measurement distance of 700 mm, the irradiance uniformity of the BB3200pg is better than ± 0.2 % in a central area with diameter of 30 mm – 40 mm [34]. The temperature stability of BB3200pg and another blackbody with similar design, BB3500, is within ± 0.2 K – 0.3 K, if a feedback stabilization system is used to control the temperature [34,35].

Storage rings

Synchrotron radiation from electron storage rings is used e.g. in X-ray absorption spectroscopy, microscopy and lithography, photoemission spectroscopy and electron microscopy, and protein analysis. Some larger NMIs utilize storage rings as spectral irradiance sources. These facilities include SURF III at National Institute of Standards and Technology (NIST, USA) [36,37], BESSY II and MLS at PTB [38,39], TROLL at All-Russian Research Institute for Optical and Physical Measurements (VNIIOFI) [40] and TERAS at National Metrology Institute of Japan (NMIJ) [41]. These sources are used especially in the UV and EUV wavelength ranges below 200 nm, where the output of a blackbody radiator is quite low [41,42]. The storage rings are typically used to calibrate secondary transfer standards, such as deuterium lamps.

A schematic of a storage ring is presented in Figure 3. In a storage ring, electrons move nearly with the speed of light. A bending magnet makes them move along a horizontal circular trajectory. The accelerated electrons emit a calculable photon flux through an aperture stop, which is placed near the tangent point of the orbital plane [43]. The spectral photon flux, which depends on the photon energy E, can be calculated with the knowledge of the electron energy W, magnetic field B, stored electron current I, effective vertical source size Σ_y, vertical emission angle Ψ, distance d between the tangent point and the aperture stop, and the area of the aperture stop, a x b, using the Schwinger equations [44],

$$\phi_E = \phi_E\left(E; W, B, I, \Sigma_y, \Psi, d, a, b\right). \tag{2}$$

The relative standard uncertainties of the calculable photon flux are around $2x10^{-3}$ [37,38,42]. The storage rings are ultrahigh vacuum systems. For a storage ring to be used as a primary source, the photon flux has to be calculable. This requires knowledge of the losses of the sealing window between the ultrahigh vacuum and the outside, as well as high-accuracy measurements and repeatability of the parameters of Eq. (2) [45]. The largest uncertainty contribution typically arises from the determination of the electron current I [37,38].

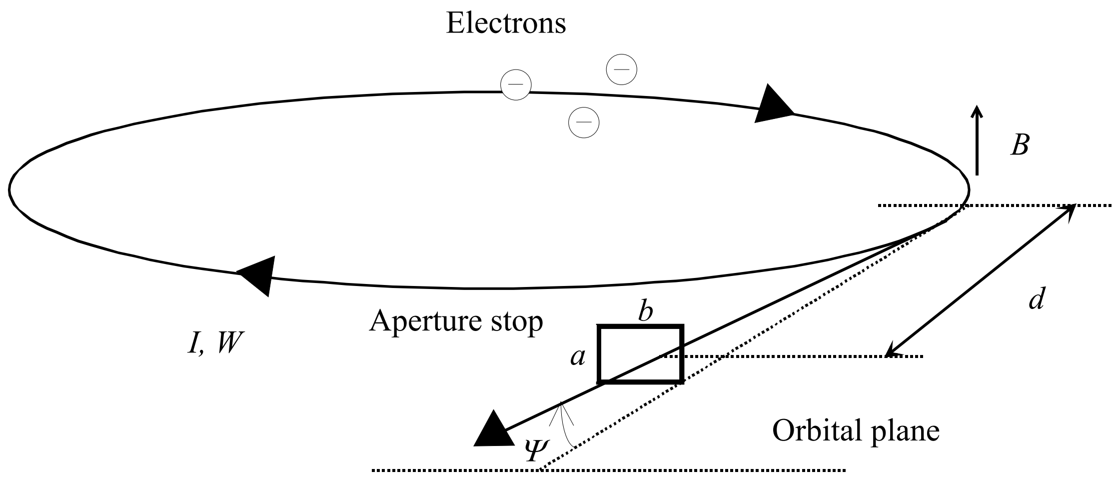

Figure 3. Schematic of a storage ring. The symbols are introduced in the text with Eq. (2).

2.1.2 Secondary radiation sources

Deuterium lamps

Deuterium arc lamps are used as spectral irradiance sources in the UV region. They provide a continuous spectrum from 180 nm to 370 nm. The operation of the lamp is started by heating the cathode for 30 – 90 seconds. The arc is produced by applying a strike voltage of over 350 V to the anode [46]. An example of a deuterium lamp is given in Figure 4.

Some deuterium lamps have been found to suffer from poor stability and reproducibility [47,48], but with careful selection, reasonable lamps can be found [49]. The typical irradiance reproducibility is within 0.4 % [49]. The ageing rate is around 7 % per 100 h [49]. The performance of the deuterium lamps can be improved by monitoring them with a suitable monitor detector, e.g. a SiC photodiode [49]. Deuterium lamps have been successfully used as transfer standards in the spectral irradiance key comparison CCPR-K1.b [21].

Figure 4. Deuterium lamp of Spectronic [50].

Tungsten halogen lamps

Tungsten halogen lamps are commonly used as transfer standards of spectral irradiance. These lamps are typically used in the wavelength range 250 nm – 2500 nm. The envelopes of the tungsten lamps are filled with halogen gas in order to extend the lifetime of the lamps with high operating temperatures. With a simple tungsten lamp, when the filament is heated, the tungsten is evaporated and attaches to the glass envelope, which causes thinning of the filament and blackening of the envelope. If halogen is added inside the lamp envelope, it evaporates as the filament heats up. The halogen atoms collide with the envelope wall and form a compound with the tungsten atoms on the wall, removing them from the envelope surface. The compound molecules move around within the envelope and dissociate if they hit the hot filament. The liberated tungsten atoms are captured back by the filament, thus regenerating it. This is called the halogen cycle [19].

The power range of the most common tungsten halogen lamps extends from 10 W to 1 kW. In this thesis, I concentrate on 1-kW FEL and DXW lamps. Examples of both lamp types are presented in Figure 5. Both lamps include a double-coiled tungsten filament. The difference between the lamp types is that the FEL lamps are single-ended, and the DXW-lamps are double-ended. The FEL lamps are typically operated with a horizontal axis, and the DXW lamps with vertical axis.

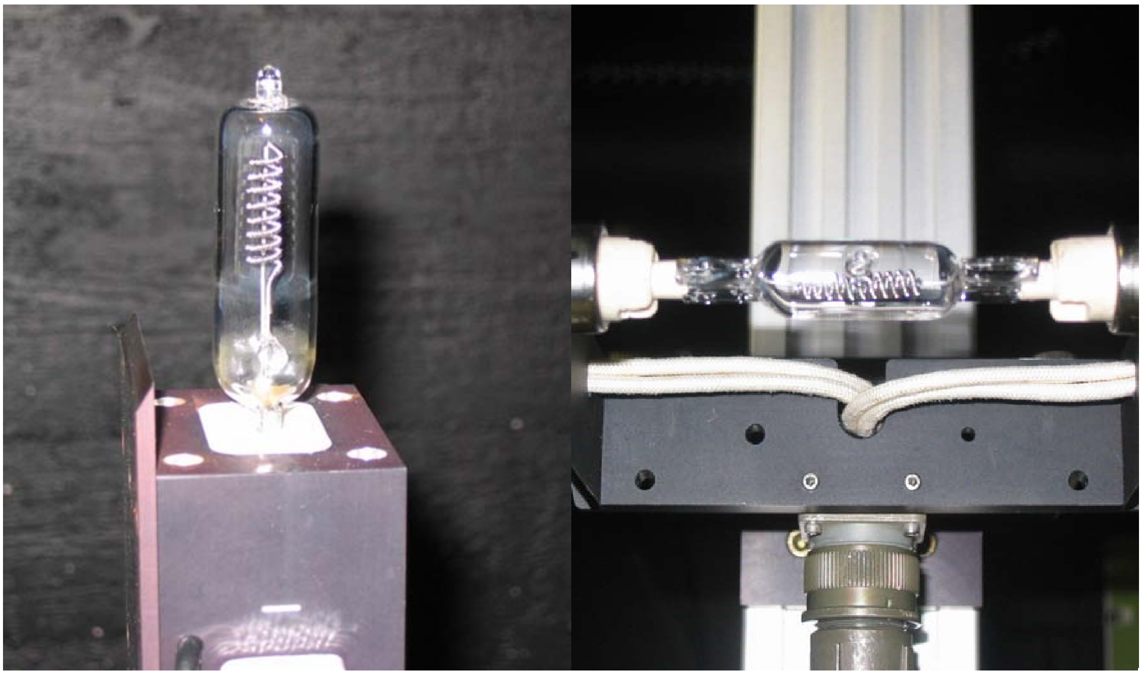

Figure 5. Lamps of types FEL (left) and DXW (right).

The properties of lamps have been studied e.g. in [51,52,53]. In [52], the irradiance uniformity of the lamp was studied by scanning the detector across the measurement plane at a distance of 500 mm from the reference plane of the lamp. The irradiance uniformity was within 0.2 % over a central area of 30 mm x 60 mm [52]. The aging rates of the lamps are around 4 % – 5 % per 100 h, when they are turned on for short periods [52,53]. Due to their compact size, incandescent lamps can be used as transfer standards in comparison measurements [22,51,54,Publ.II,Publ.III]. The lamps have to be transported with care as they are sensitive to shocks during transportation [51,52].

The lamps have spectrally varying emissivities. The emissivity of the tungsten filament is the main component influencing the effective emissivity of a lamp. The emissivity of tungsten plate has been determined by e.g. de Vos [24] and Larrabee [55]. Dmitriev *et al* determined the emissivity of a tungsten strip [56,57]. The transmittance of the glass bulb, absorption of the filling gas [58,59], light recycling in the coiled filament [60,61] and possible impurities of the filament have smaller effects on the effective emissivity. The emissivity of the lamp can be modeled using an N^{th}-degree polynomial of the form,

$$\varepsilon = \sum_{j=0}^{N} b_j \lambda^j , \tag{3}$$

where the degree N typically varies between 3 and 7 [10,11,62,63,64,65]. Even a first-degree model has been proposed for a limited wavelength range [66]. Polynomial emissivity models used for interpolation require several spectral irradiance data points to avoid oscillations between the wavelengths of the measured points.

2.1.3 Tungsten lamp as absolute source

In [Publ.I], I present a spectral irradiance model for a tungsten halogen lamp. The model is based on Planck's radiation law [Eq. (1)], emissivity of tungsten filament determined by de Vos [24] in polynomial form [25], and a residual correction function, which takes into account the other factors affecting the spectral emissivity. The spectral irradiance of the lamp is modeled as

$$E(\lambda,T) = B(T)\varepsilon_{\mathrm{W}}(\lambda,T)\varepsilon_{\Delta}(\lambda,T)L(\lambda,T), \tag{4}$$

where $\varepsilon_W(\lambda,T)$ is the emissivity of the tungsten filament, and $\varepsilon_\Delta(\lambda,T)$ is a correction function for taking into account other spectrally varying non-idealities of the lamp. $L(\lambda,T)$ is the blackbody radiance from Eq. (1). Parameter $B(T)$ is a geometrical factor, which takes into account the measurement distance and the dimensions of the filament. Temperature affects $B(T)$ only through thermal expansion of the dimensions of the filament [67,68].

The correction function $\varepsilon_\Delta(\lambda,T)$ was determined for the wavelength range 340 nm – 850 nm by measuring the spectral irradiance of an FEL lamp at five different operating temperatures between 2500 K and 3050 K. The correction function was calculated by dividing the measured spectral irradiances $E_m(\lambda,T)$ by the product of the blackbody radiance, emissivity of tungsten and the geometrical factor,

$$\varepsilon_\Delta(\lambda,T) = \frac{E_\mathrm{m}(\lambda,T)}{L(\lambda,T)\varepsilon_\mathrm{W}(\lambda,T)B(T)}. \tag{5}$$

The spectral shape of the correction function is almost the same for all temperatures [Publ.I]. Figure 6 presents the average of the normalized correction functions, and an 8^{th} -degree polynomial fitted to the average. The 8^{th} -degree polynomial was taken into use as a temperature independent correction function $\varepsilon_\Delta(\lambda)$. The coefficients of the polynomial are given in [Publ.I]. A polynomial is not necessarily the best fitting function in general, because of the risk of large deviations at the ends of the fitting intervals, making it unsuitable for extrapolation, in particular. Therefore, a rational function is sometimes better because it behaves more smoothly. However, for the purpose at hand, the polynomial used here proved to be adequate, especially when not extrapolating outside the measurement region. After determining the correction function $\varepsilon_\Delta(\lambda)$ for a lamp, the spectral irradiance can be determined using only two or three measurement points. In [Publ.I], the model was validated with incandescent lamps of types FEL and DXW previously calibrated by TKK and National Physical Laboratory (NPL, UK). The results agree within 1 %.

The developed model can be used to determine a simple (absolute) spectral irradiance scale, if the temperature of the filament and an absolute measure of the spectral irradiance are known [Publ.I]. The temperature of the lamp filament can be obtained either from the color temperature of the lamp, or from the hot and cold resistance measurements of the lamp filament. In both cases, the absolute measure of the spectral irradiance may be obtained from an illuminance measurement.

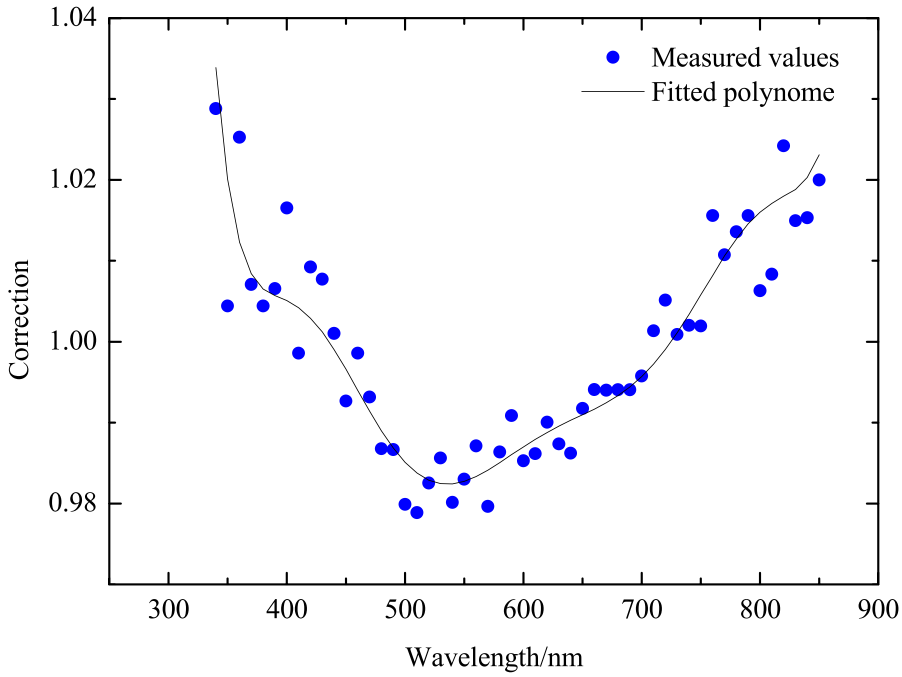

Figure 6. Measured values for the correction function $\varepsilon_{\Delta}(\lambda)$ and an 8^{th} -degree polynome fitted to the results. The correction describes the effects of non-idealities such as transmittance of the glass bulb, absorption of the filling gas and light recycling on the lamp irradiance.

The color temperature of a lamp may be obtained by measuring the lamp with a colorimeter, or it may be known from manufacturer's specifications. The relation between the color temperature and the physical temperature of the filament may be determined using the method described in [69]. Using resistance measurements at room temperature and at burning temperature, the temperature of the filament may be obtained from the known temperature dependence of the resistance of tungsten [70,71,72]. In the temperature range 2400 K – 3200 K, the temperature of the filament can be calculated as

$$T = \frac{R(T)}{0.0062\mathrm{K}^{-1} R(295\mathrm{K})} + 319\mathrm{K}, \qquad (6)$$

where $R(T)$ is the hot resistance and $R(295\ \mathrm{K})$ is the room temperature resistance. With typical measurement uncertainties of color temperature and illuminance, 20 K and 2 %, uncertainties of 2 % to 3 % in spectral irradiance can be obtained [Publ.I].

2.2 Spectral irradiance scale realizations

Spectral irradiance scales may be based on a primary source (blackbody or synchrotron radiation). The spectral irradiance of the source could be determined directly, e.g. via an ITS-90 temperature measurement and Planck's radiation law [Eq. (1)] or current measurements and Schwinger's law [Eq. (2)]. Another alternative is to determine the irradiance via optical means traceable to the absolute cryogenic radiometer. The cryogenic radiometer can be used to calibrate filter radiometers or transfer standard detectors [73].

Absolute cryogenic radiometers are operated at temperatures typically below 20 K [9]. That improves their sensitivity and accuracy by a factor of 100 compared with the operation at room temperature [73]. The calibrations carried out with cryogenic radiometers provide relative uncertainties better than 10^{-4} [9]. Cryogenic radiometers are based on electrical substitution principle. The temperature rise of a detector is measured relative to a constant-temperature reference heat sink during alternate radiant and electrical heating cycles. The electrical power is adjusted in such a way that the detector temperature rise is equal to the heating caused by the radiant power in order to equate the radiant power to the measured quantity of the electrical power. The detector element is a cavity, which absorbs nearly all of the incoming radiation. The radiation beam enters into the cavity after passing through an entrance window at the Brewster angle [73]. As radiation sources, laser lines [23,73,74,75] or monochromators [76,77] may be used. The laser-based applications typically provide smaller uncertainties, but the monochromator-based applications are more versatile [77]. The electrical heating may be carried out using resistive heaters [73,74].

In the wavelength range 250 nm – 2500 nm, the spectral irradiance scales of PTB [78], NPL [33] and NIST [12] combine measurements based on blackbodies and cryogenic radiometers. The thermodynamic temperature of an HTBB is determined with filter radiometers calibrated traceable to a cryogenic radiometer. The output radiation of the HTBB is then calculated according to Eq. (1). National Research Council (NRC, Canada) is also developing this type of spectral irradiance scale [79]. In the realization of the scale of Korea Research Institute of Standards and Science (KRISS) [80], the temperature of an HTBB is determined using a detector calibrated with temperature scale based on the ITS-90.

Alternatively, detector approaches traceable to the cryogenic radiometer can be used directly to obtain a spectral irradiance scale via filter radiometry of secondary sources or responsivity measurements of a spectroradiometer. Tungsten halogen lamps are used as light sources in the scales based on detectors traceable to cryogenic radiometers e.g. at Instituto de Física Aplicada – Consejo Superior de Investigaciones Científicas (IFA-CSIC, Spain) [81,82], in NRC's present scale [64,79,83], MIKES/TKK [10,11], and Ulusal Metroloji Enstitüsü (UME, Turkey) [84]. As the lamps are not Planckian radiators, measurements at multiple wavelengths are required. To facilitate the measurements, the filter radiometers may be built to utilize interchangeable filters [85]. Changing the filter can also be automated [Publ.II].

In Nederlands Meetinstituut – Van Swinden Laboratorium (NMi-VSL, the Netherlands), a monochromator based cryogenic radiometer is used to calibrate a spectroradiometer. The spectroradiometer consists of a double monochromator and an integrating sphere with a diameter of 5 cm as entrance port. To calibrate the spectroradiometer, radiation from the double monochromator in conjunction with the cryogenic radiometer is redirected to the double monochromator of the spectroradiometer. The spectroradiometer is placed on a rotary stage, so that it can be rotated to measure unknown radiation sources directly after calibration [86].

2.3 Spectral irradiance scale of MIKES/TKK

The primary spectral irradiance scale realization of MIKES/TKK is described in [10,11]. The scale is based on filter radiometers and tungsten halogen lamps. The construction of the filter radiometers is described in [85]. The filter radiometer consists of a trap detector of three silicon photodiodes, a precision aperture, a set of 14 interchangeable, temperature-stabilized, narrow-band interference filters, and a broadband $V(\lambda)$–filter. The components of the filter radiometer are characterized separately [10]. The spectral responsivity of the trap detector is measured traceably to a cryogenic radiometer. The precision aperture is calibrated using an optical co-ordinate measurement machine [87]. The filter transmittances are measured using a commercial double-beam monochromator, the performance of which is routinely checked with a reference spectrometer [88].

The alignment of the equipment for spectral irradiance measurements is shown in Figure 7. The filter radiometer and the lamp are aligned on an optical rail with help of a dual-beam alignment laser. The distance is set with aid of a magnetic distance measurement system. The system consists of a magnetic ruler attached on a rail, a detector attached on a carriage on top of which the filter radiometer is installed, and a display unit. The magnetic length scale is calibrated with a laser interferometer.

The photocurrents are measured for each filter. The relation between the photocurrent i_{ph} and the spectral irradiance $E(\lambda)$ is

$$i_{ph} = A\int R(\lambda)\tau(\lambda)E(\lambda)\,d\lambda\,, \tag{7}$$

where A is the area of the aperture, $R(\lambda)$ is the responsivity of the trap detector and $\tau(\lambda)$ is the transmittance of the filter. $E(\lambda)$ is calculated using Eq. (1), with emissivity ε calculated using Eq. (3) with $N = 7$. In the calculation of $R(\lambda)\tau(\lambda)$, correction for interreflections between the trap detector and the filter is taken into account.

The photocurrent is calculated for each filter at its effective wavelength with the initialization values for T, B, and $\varepsilon(\lambda)$. For the initialization values of $\varepsilon(\lambda)$, emissivity data of de Vos [24] are used. The spectral irradiance values corresponding to each effective wavelength are calculated using a recursive process of minimizing the differences between the calculated and measured photocurrents by adjusting the values of T, B, and $\varepsilon(\lambda)$. As the result, spectral irradiance values at the effective wavelengths of the filter, continuous spectral irradiance, and values for T, B and $\varepsilon(\lambda)$, are obtained.

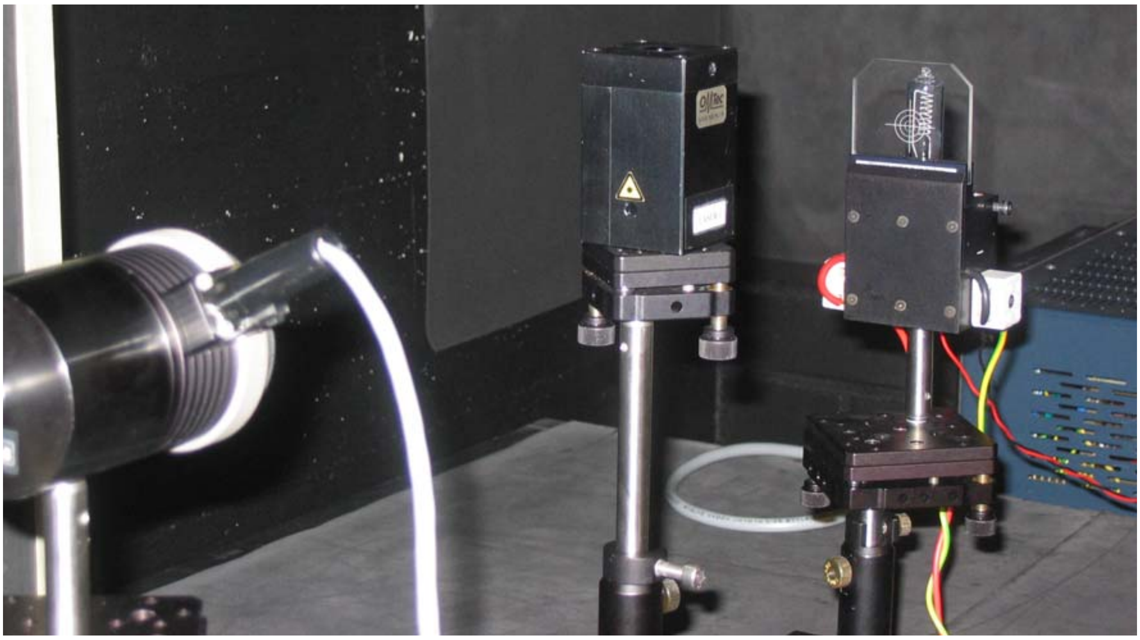

Figure 7. Alignment of the filter radiometer and an FEL lamp. Devices from left to right: Filter radiometer, alignment laser, lamp with an alignment target and power supply.

2.4 Comparisons of the spectral irradiance scales

Comparison measurements are frequently carried out to validate the quality of the national calibration services. In order to provide all NMIs the opportunity to participate, different types of comparisons are needed.

Figure 8 presents the scheme for key comparisons. The key comparisons of the CIPM have a few participants from each regional metrology organization (RMO). It has been agreed that only the CIPM key comparisons provide the KCRVs. All NMIs are offered a possibility to link their measurement results to the KCRVs through bilateral and regional key comparisons with linking laboratories that have taken part in the CIPM key comparison. The KCRV for spectral irradiance was determined in the key comparison CCPR-K1.a [20], which was carried out during years 2000 – 2004.

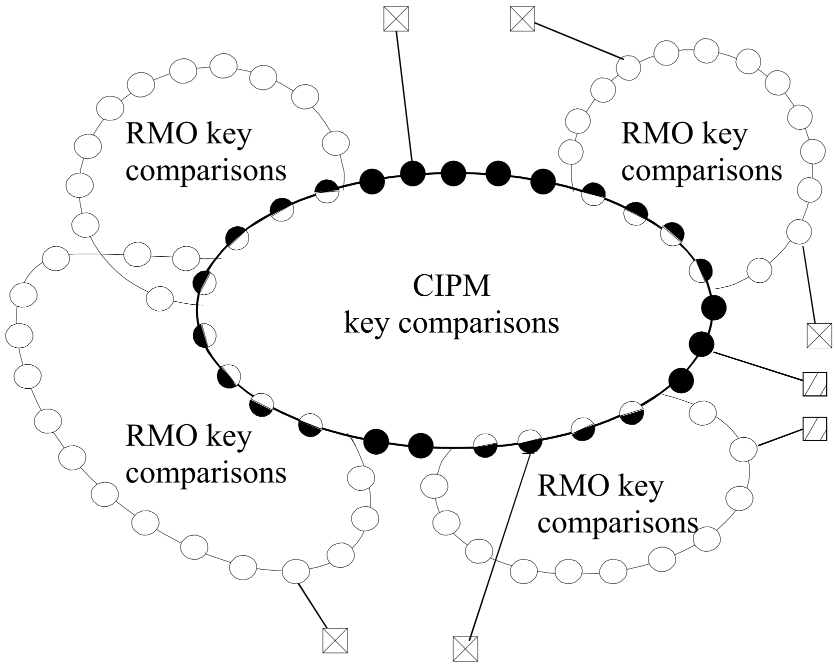

●NMI participating in CIPM key comparisons
◐NMI participating in CIPM key comparisons and in RMO key comparisons
○NMI participating in RMO key comparisons
⊠NMI participating in a bilateral key comparison
▨International organization signatory to the Mutual Recognition Arrangement (MRA)

Figure 8. Scheme for key comparisons [89].

In addition to the CCPR-K1.a, MIKES/TKK has participated in several other comparison measurements in spectral irradiance during recent years [54,90,Publ.II,Publ.III]. The scales of MIKES/TKK and NMC were compared in autumn 2007 using NMC's new multi-wavelength filter radiometer (MWFR) facility [Publ.II]. The measurement setup is shown in Figure 9. It comprises 24 filters, Si and InGaAs detectors, and a 4-mm precision aperture. Three tungsten halogen lamps, one from MIKES/TKK and two from NMC, were measured. The MIKES/TKK lamp was measured at TKK before and after it was transported to NMC. The scales of MIKES/TKK and NMC showed good agreement [Publ.II].

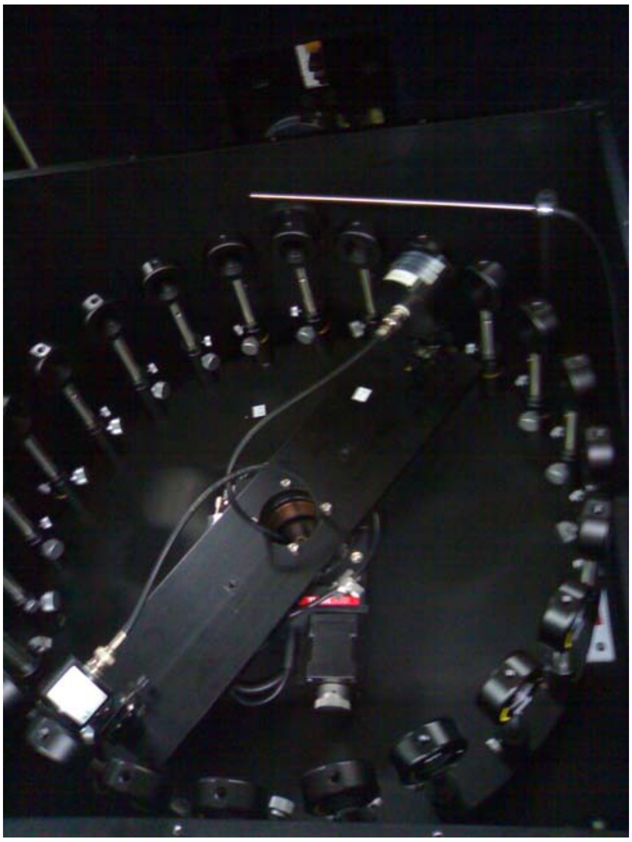

Figure 9. The MWFR facility of NMC. The Si and InGaAs detectors are placed on the central rotary stage. The 24 filters are placed on the outermost rotary stage.

The long-term reproducibility of the scales can be studied by comparing the mutual degrees of equivalence (DoE) obtained in different comparisons. If the scales remained stable, the difference of the DoEs should be close to zero. To study the long-term reproducibility of MIKES/TKK, data from the comparison reported in [Publ.II] and the key comparisons CCPR-K1.a [20] and CCPR-K1.a.1 [26] were used. As can be seen in Figure 10, the agreement, and thus the long-term stability, is good in the wavelength range above 400 nm. The difference below 400 nm is somewhat larger, up to 2.8 %, though still within the expanded uncertainties of the comparison. The expanded uncertainties of the comparison were calculated as quadratic sums of the expanded uncertainties of MIKES/TKK and NMC. The long-term stability information obtained from this comparison is discussed in [Publ.III].

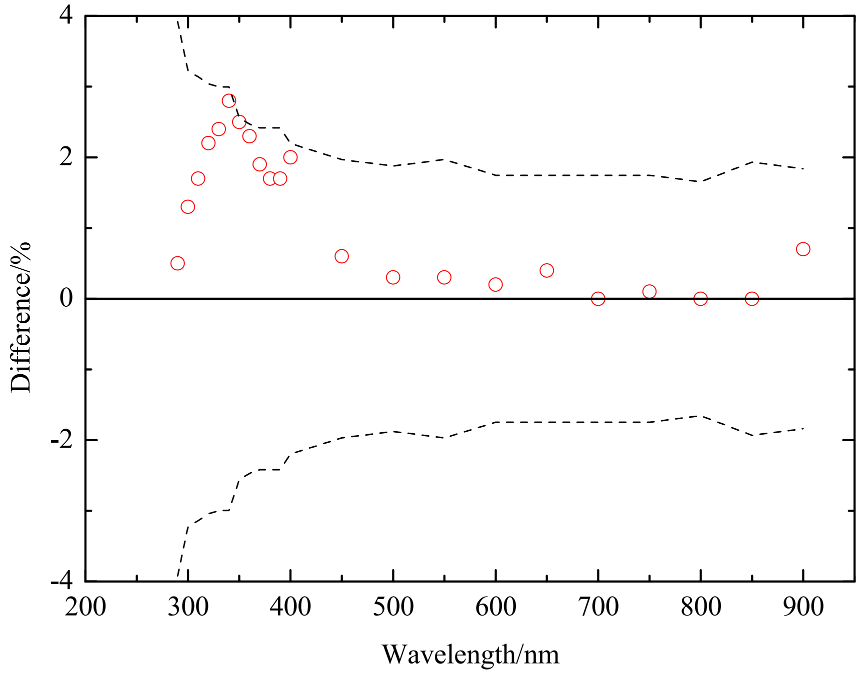

Figure 10. Long-term reproducibility of the difference of the spectral irradiance scales of NMC and MIKES/TKK. The reproducibility information has been obtained by comparing the results of [Publ.II], CCPR-K1.a [20] and CCPR-K1.a.1 [26].The dashed lines represent the expanded uncertainty of the comparison of [Publ.II].

2.5 Uncertainty evaluation in linking key comparisons

An NMI can be linked to the KCRV through a bilateral or a regional key comparison with another NMI which has participated in the CIPM key comparison. The linking process has been studied in different fields of metrology [91,92,93,94,Publ.III].

In the spectral irradiance key comparison CCPR-K1.a, the participants reported two types of uncertainties associated with either correlated or uncorrelated effects in the measurements. The contributions associated with the correlated effects reproduce their values systematically from one measurement to another, while the uncorrelated contributions vary randomly, either between the individual measurements or between the measurement rounds. The separation of the uncorrelated effects from the combined uncertainty is useful for the uncertainty evaluation in linking the results of different comparisons, as the additional uncertainty due to linking can be estimated more realistically [Publ.III].

In [22,Publ.III], the results of NIMT are linked through MIKES to the KCRV obtained in CCPR-K1.a [20]. The described method takes into account the uncertainty of the linked NMI, uncertainties associated with the uncorrelated effects in the measurements of the linking NMI, transfer uncertainties of the bilateral and the CIPM comparisons, uncertainty of the KCRV, and the uncertainty associated with the long-term reproducibility of the linking NMI.

In order to describe the concepts more generally, the notation here does not apply just to spectral irradiance. The measured value (measurement result, e.g. spectral irradiance) is described by Ξ and the errors as E. According to *Guide to the Expression of Uncertainty in Measurement* (GUM) [95], the capital letters denote random variables, whereas the lowercase letters denote the corresponding expectation values. The key comparison measurement by an NMI i is subject to errors related to uncorrelated and correlated effects in the measurements, as well as artifact instability during transportation and errors in the transfer of the primary scale to transfer standards. The measurements in bilateral comparisons are subject to similar errors. If the time between the key comparison and the bilateral comparison is long, the reproducibility of the linking scale needs also to be taken into account. One may also be interested in calculating mutual DoE for the linked NMI and another NMI j, which has also participated in the key comparison but is not involved with the linking process.

The unilateral DoEs $D_{\alpha(i)}$ of the linked NMI α are calculated as

$$D_{\alpha(i)} = \Xi_{\alpha} + I_i - X_{\mathrm{ref}} + E_{\mathrm{kc},i} + E_{\mathrm{b},i} + E_{\mathrm{r},i} \tag{8}$$

where Ξ_α is the measurement result of the linked NMI, I_i is the linking invariant [93], which corresponds to changes of the true value of the measurand, in case the linking NMI utilizes different measurand artifacts in the different comparisons. The linking laboratory links the measured value of the artifact used in the bilateral comparison to that used in the key comparison through its own measurements. Parameter X_{ref} is the KCRV. $E_{\mathrm{kc},i}$ is the transfer error term from the key comparison for the linking NMI. The transfer error is related to artifact instability during transportation, and transfering the primary scale to transfer standards of the comparison. $E_{\mathrm{b},i}$ combines the transfer error of the bilateral comparison and the error related to uncorrelated effects of the linking NMI during the comparison. $E_{\mathrm{r},i}$ is the error term associated with the reproducibility of the linking NMI between the key comparison and the bilateral comparison.

The corresponding uncertainties $u(d_{\alpha(i)})$ of the linked NMI are calculated as

$$u^2\left(d_{\alpha(i)}\right) = u_\alpha^2 + u^2\left(x_{\mathrm{ref}}\right) + \left(1 - 2w_i\right) u_{\mathrm{kc}}^2 + u_{\mathrm{b},i}^2 + u_{\mathrm{r},i}^2, \tag{9}$$

where u_α corresponds to the standard uncertainty of the linked NMI, $u(x_{\mathrm{ref}})$ is the uncertainty of the KCRV, u_{kc} is the transfer uncertainty of the CIPM key comparison, w_i is the weight of the linking NMI, $u_{\mathrm{b},i}$ is the uncertainty of the bilateral comparison, and $u_{\mathrm{r},i}$ is the uncertainty due to the long-term reproducibility of the scale of the linking NMI. Equation (9) takes into account the correlation between the KCRV and the transfer error associated with the measurements of the linking NMI. The correlation is caused by the fact that the linking NMI's results were used to calculate the KCRV.

The mutual DoEs with an NMI j, $D_{\alpha j}$, and the corresponding uncertainties $u(d_{\alpha j})$ are calculated as

$$D_{\alpha j} = D_{\alpha(i)} - D_j = \Xi_\alpha - \Xi_j + I_i - E_{\mathrm{kc},j} + E_{\mathrm{kc},i} + E_{\mathrm{b},i} + E_{\mathrm{r},i} \tag{10}$$

and

$$u^2\left(d_{\alpha j}\right) = u_\alpha^2 + u_j^2 + 2u_{\mathrm{kc}}^2 + u_{\mathrm{b},i}^2 + u_{\mathrm{r},i}^2 \qquad (11)$$

where D_j is the degree of equivalence of NMI j, Ξ_j is the measurement result of NMI j, $E_{\mathrm{kc},i}$ is the transfer error term from the key comparison for participant j, and u_j is the uncertainty associated with uncorrelated effects between the measurements of NMI j. The detailed derivations of Eqs. (8 – 11) are presented in [Publ.III].

Figure 11 shows the contribution of the different uncertainty components to the combined standard uncertainty of NIMT DoE at different wavelengths. In order to reduce the overall uncertainty, NMIs with small uncertainties associated with uncorrelated effects in the measurements should be favored when selecting the linking NMI. In this case, the uncertainty associated with uncorrelated effects in the measurements of NIMT contributes the most in the combined standard uncertainty [Publ.III].

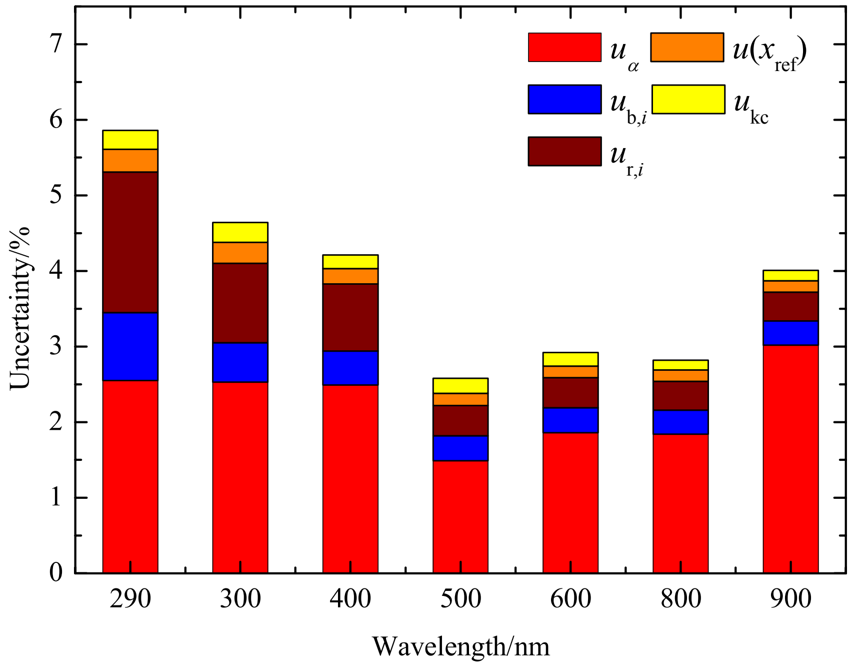

Figure 11. The contribution of the different uncertainty components to the overall uncertainty of the DoEs of NIMT. u_α = standard uncertainties of NIMT, $u_{b,i}$ = transfer uncertainties of the bilateral comparison, $u_{r,i}$ = uncorrelated uncertainties of MIKES including the long-term reproducibility of the scale, $u(x_{ref})$ = uncertainties of KCRV, u_{kc} = transfer uncertainties of the CIPM key comparison.

3 Radiation temperature

3.1 The International Temperature Scale of 1990

Thermodynamic temperature is the absolute measure of temperature. The SI unit of the temperature, kelvin, is defined to be 1/273.16 of the thermodynamic temperature of the triple point of water (273.16 K). Direct measurements of the thermodynamic temperature are not always straightforward, and in order to assist the practical calibrations and measurements, international temperature scales based on auxiliary fixed temperature points have been defined.

The ITS-90 is established by several fixed temperature points given in Table 1. The fixed points have been determined by measuring the thermodynamic temperatures of the corresponding phase transitions as accurately as possible at the time being [2]. The values between the fixed points are obtained by using agreed interpolation functions and artifacts. Due to the method of realization, there are known discrepancies between the thermodynamic temperatures and the ITS-90 temperatures.

Table 1. Defining fixed points of the ITS-90 [2]. V = vapor pressure point, T = triple point, G = gas thermometer point, M = melting point, F = freezing point.

Number	Temperature T_{90}, K	t_{90}, °C	Substance	State
1	3 to 5	-270.15 to -268.15	He	V
2	13.8033	-259.3467	e-H_2	T
3	≈17	≈-256.15	e-H_2 (or He)	V (or G)
4	≈20.3	≈-252.85	e-H_2 (or He)	V (or G)
5	24.5561	-248.5939	Ne	T
6	54.3584	-218.7916	O_2	T
7	83.8058	-189.3442	Ar	T
8	234.3156	-38.8344	Hg	T
9	273.16	0.01	H_2O	T
10	302.9146	29.7646	Ga	M
11	429.7485	156.5985	In	F
12	505.078	231.928	Sn	F
13	629.677	419.527	Zn	F
14	933.473	660.323	Al	F
15	1234.93	961.78	Ag	F
16	1337.33	1064.18	Au	F
17	1357.77	1084.62	Cu	F

The temperatures between the fixed points are determined by interpolating instruments, such as resistance thermometers, gas thermometers and pyrometers [2]. After its implementation, the ITS-90 has been supplemented by the Provisional Low Temperature Scale (PLTS-2000) from 0.9 mK to 1 K [96]. Several of the temperature determination ranges overlap, and thus differing definitions of the ITS-90 exist. These differing definitions are given equal status [2].

The temperatures in the range from 0.65 K to 5 K are realized using vapor pressure relations of ^{3}He and ^{4}He. A vapor pressure thermometer consists of a vessel containing liquid in equilibrium with its vapor. The equations for the vapor pressure of He and the corresponding temperature are given in [30] for ranges of 0.65 K to 3.2 K for ^{3}He, 1.25 K to 2.1768 K for ^{4}He and 2.1768 K to 5 K for ^{4}He.

From 3 K to 24.5561 K (Ne triple point) the temperature is realized using constant volume ^{3}He and ^{4}He gas thermometry. A constant volume gas thermometer consists of a bulb filled with gas. The volume of the gas is constant. The pressure of the gas varies with temperature and it is measured with a manometer. The equations relating temperature and pressure are given in [2,30]. The thermometer is calibrated at three temperatures: at the triple point of Ne, at the triple point of equilibrium H_2, and at a third temperature point selected from the interval between 3 K and 5 K. The temperatures between 3 K and 5 K are determined using a He vapor pressure thermometer. In measurements below 4.2 K, the non-ideality of the gas must be taken into account [30].

The temperatures between 13.8033 K and 1234.93 K are realized using platinum resistance thermometers (PRTs). The resistance thermometers are based on the temperature dependent change of the resistance of platinum. There are three types of PRTs widely used: capsule thermometers, which are used as standard interpolation instruments between 13.8 K and 273.16 K, long-stem low or medium temperature thermometers (between 84 K and 933 K) and long-stem high temperature thermometers (up to 1234 K) [30]. At the lower part of the scale, the sensitivity of the resistance becomes small, which acts as the limiting factor. At high temperatures, the critical factors include the prevention of the electrical leakage, maintaining cleanliness and preventing the detector from contamination.

The PRTs are calibrated at specified sets of fixed points. The temperature range determined using PRTs is divided into subranges [2,30]. The temperatures are determined in terms of the resistance ratios,

$$W(T_{90}) = \frac{R(T_{90})}{R(273.16\ \mathrm{K})}, \tag{12}$$

where $R(T_{90})$ is the resistance at temperature T_{90}, and R(273.16 K) is the resistance of the PRT at the triple point of water. The T_{90} is determined from the $W(T_{90})$ using specified reference functions [2,30].

Above the freezing point of silver, the ITS-90 is based on Planck's radiation law [Eq. (1)]. The temperature T_{90} is determined using the ratio of the radiance at the unknown temperature to that measured at a fixed temperature,

$$\frac{L(\lambda, T_{90})}{L[\lambda, T_{90}(x)]} = \frac{\exp\left[\frac{c_2}{\lambda T_{90}(x)}\right] - 1}{\exp\left(\frac{c_2}{\lambda T_{90}}\right) - 1}, \tag{13}$$

where $T_{90}(x)$ is the freezing point of either silver (1234.93 K), gold (1337.33 K) or copper (1357.77 K), $L[\lambda, T_{90}(x)]$ is the corresponding radiance, $L(\lambda, T_{90})$ is the radiance at the temperature T_{90}, λ is the wavelength and c_2 is the second radiation constant defined by the Committee on Data for Science and Technology (CODATA). The measurements are carried out using optical measurement devices, pyrometers.

3.2 Trends for the international temperature scale

In the ITS-90, there are no fixed temperature points above the copper freezing point, 1357.77 K. The scale is purely extrapolated using Planck's radiation law [Eq. (1)]. This method is vulnerable to extrapolation errors [Publ.IV] and propagation of uncertainties [97,98,99,100]. The uncertainty propagates as the square of the temperature difference to the reference temperature [101].

The Consultative Committee for Thermometry - Working Group 5 (CCT-WG5) is currently reviewing the possibility of suggesting direct methods for measuring thermodynamic temperature, rather than using ITS-90. Initial work indicates that determining the thermodynamic temperatures using optical power and length measurements, could obtain measurement uncertainties lower than those of ITS-90 [97,102]. NIST has reported expanded measurement uncertainties of ± 0.110 K and ± 0.129 K for measurements of the thermodynamic temperatures of silver and gold freezing points [13]. NPL has obtained corresponding uncertainties of ± 44 mK and ± 49 mK [14]. The measurement results of NIST and NPL agree within uncertainties [13,14]. The corresponding uncertainties of ITS-90 are ± 80 mK for silver and ± 100 mK for gold freezing points [30]. At PTB, measurements at Zn and Al fixed points (629.677 K and 933.473 K) have been carried out with uncertainties of 29 mK and 52 mK using an InGaAs detector [16]. Possible detector materials for lower temperatures are e.g. InGaAs (lowest measurable fixed point 692 K), NIR-extended InGaAs (429 K) and InSb (273 K) [97].

Research aiming at finding auxiliary high temperature fixed points above the Cu freezing point is also being carried out. According to the recommendation of CCT and CCPR (Consultative Committee for Photometry and Radiometry), the reproducibility of the new high temperature fixed points should be within 100 mK [103]. Instead of pure metal, the high temperature fixed points consist of a eutectic or peritectic mixture of two materials. Pure metals can not be used as fixed points at higher temperatures, because graphite used as crucible material contaminates pure metals. Using metal-carbon (M-C) eutectic alloys provides a solution to the contamination problem. If the carbon is an integral part of the eutectic alloy, a graphite crucible can be used [104].

The eutectic point is the lowest temperature point at which a single liquid phase can exist in the composition of two materials. At the eutectic point, there are three phases present: solid phases of both materials, and a liquid phase of the mixture. This temperature value is unique. The research has focused on Re-C (eutectic point at 2747 K), Ru-C (2227 K), Pt-C (2011 K), Pd-C (1765 K) and Co-C (1597 K) cells [3,105]. The temperature range can be extended up to 3500 K with metal-carbide-carbon (MC-C) eutectics, for example with TiC-C (3034 K), ZrC-C (3156 K), or HfC-C (3458 K) [4].

The thermodynamic temperatures of the Co-C, Pd-C, Pt-C and Ru-C eutectic fixed points have been determined with the expanded uncertainty of 400 mK [3]. A 100-mK reproducibility between different cells can be reached with adequate filling arrangements [106]. The repeatability of one single cell is better than 70 mK [4]. The structure of a MC-C fixed point cell is presented in Figure 12.

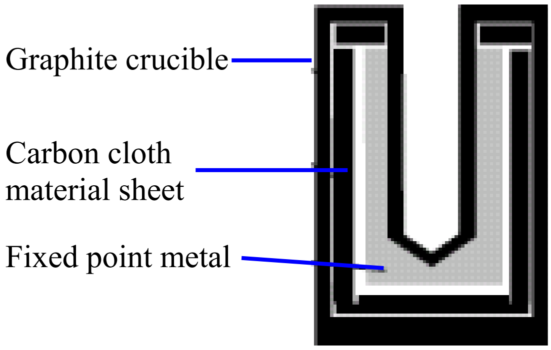

Figure 12. Structure of a MC-C fixed point cell [4].

Peritectic temperature is the highest temperature at which a single solid carbide phase can exist. At the peritectic point, the solid metal-carbide is in equilibrium with the solid carbon and the liquid metal-carbide. The studied and reported compositions are Mn_7C_3-C (peritectic point at 1606 K) [5], Cr_3C_2-C (2099 K) [5,6,7] and WC-C (3022 K) [5,8]. The reproducibility has been reported to be of the same quality as for the eutectics, even though the purity of the metal used in the peritectics is lower [5].

High temperature fixed point cells have problems related to their short lifetimes and lack of suitable blackbody furnaces. Temperature uniformity of the furnace is important for the reproducibility of the transition temperature and the quality of the plateau [4]. Mechanical stress caused by thermal expansion reduces the lifetime of the fragile cells [4]. During the construction, the cell is extremely vulnerable to contamination [106]. The contamination may be due to impurities in the metal, contaminated graphite or cross-contamination during the filling process. Cross-contamination can be reduced by proper purifying of the fixed point cell furnace tubes between manufacturing different fixed point cells, or by using separate furnace parts for different fixed point materials [106].

3.3 Radiation temperature scale of MIKES

The MIKES radiation temperature measurement facility includes an LP3 linear radiation thermometer [107] manufactured by KE Technologie GmbH, and two filter radiometer housings, labeled FR1 and FR2. Pictures of the measurement equipment are presented in Figure 13.

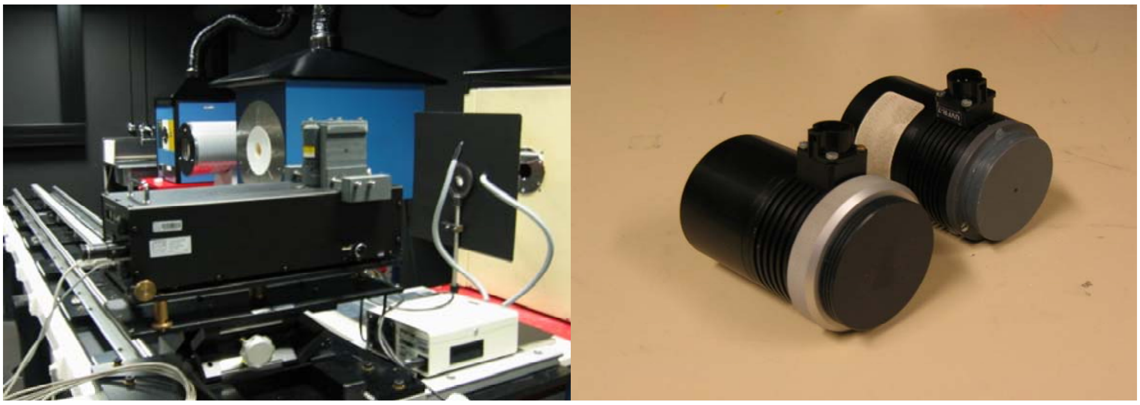

Figure 13. Linear radiation thermometer LP3 and the filter radiometer housings FR1 and FR2.

The LP3 consists of a Si photodiode, imaging optics, and band pass filters with nominal pass band center wavelengths of 650 nm and 900 nm. In this study, the band pass filter with the nominal wavelength of 650 nm is used. To calibrate the device, an ITS-90 fixed point cell, either Ag or Cu, is measured and the corresponding photocurrent i_{cal} is recorded. The target with unknown temperature is then measured and photocurrent i_{ph} is recorded. The unknown temperature of the target is obtained as

$$T = \left[\frac{1}{T_{90}} - \frac{\lambda_{eff}}{c_2} \ln \frac{i_{ph}}{\zeta \cdot i_{cal}} \right]^{-1}, \tag{14}$$

where c_2 is the second radiation constant defined by CODATA, T_{90} is the reference temperature used in the calibration of the radiation thermometer, and $\xi = \kappa\varepsilon\tau\rho$ combines the attenuation κ, emissivity ε, transmittance of the filter τ and the reflectance ρ of the optical components. Parameter λ_{eff} is the effective wavelength of the pyrometer. It is calculated using the Wien approximation,

$$\lambda_{\mathrm{eff}} = \frac{c_2\left(\frac{1}{T_1} - \frac{1}{T_2}\right)}{\ln\left(\frac{s(T_2)}{s(T_1)}\right)}, \tag{15}$$

where T_1 and T_2 are two temperatures defined by ITS-90, and $s(T_1)$ and $s(T_2)$ are the corresponding recorded pyrometer signals.

The construction of the filter radiometer FR1 is described in [85] and FR2 in [108]. FR1 utilizes three interchangeable filters: two narrow-band interference filters with nominal pass band center wavelengths of 800 nm and 900 nm, and a $V(\lambda)$–filter. FR2 includes a fixed filter at the nominal pass band center wavelength of 800 nm. The characterization of the FR1 is described in [85] and of the FR2 in [109].

The relation between the blackbody radiance $L(\lambda,T)$ and the photocurrent i_{ph} produced by the filter radiometer is

$$i_{\mathrm{ph}} = \frac{A_{\mathrm{BB}}\left(1 + \frac{r_{\mathrm{BB}}^2\, r_{\mathrm{FR}}^2}{D^4}\right)}{D^2}\varepsilon\int S(\lambda)\, L(\lambda,T)\, d\lambda\,, \tag{16}$$

where $L(\lambda,T)$ is the blackbody radiation from Eq. (1), $S(\lambda)$ is the spectral irradiance responsivity of the filter radiometer, and λ is the wavelength. A_{BB} is the aperture area of the blackbody, r_{BB} is the radius of the blackbody aperture, r_{FR} is the radius of the filter radiometer aperture, and ε is the emissivity of the blackbody. The geometric factor D is defined as

$$D^2 = d^2 + r_{\mathrm{BB}}^2 + r_{\mathrm{FR}}^2 , \tag{17}$$

where d is the distance from the filter radiometer aperture to the blackbody aperture. The factor takes into account the measurement geometry related to the distance and the areas of the apertures. Temperature T is obtained from the measured photocurrent by minimizing the difference between the theoretical current, calculated using Eq. (16), and the measured current, by adjusting iteratively the temperature in Eq. (1). At first, the temperature is set to an initialization value, e.g. to the fixed point temperature defined by ITS-90, or to the pyrometer reading.

The radiation temperature measurements at MIKES have focused in the measurements of Cu and Ag fixed point cells, and comparison measurements of a VTBB with the LP3 in the range 1370 K – 1770 K [110,111,Publ.IV]. The measurement setup is presented in Figure 14. In the early stage of the VTBB measurements, the linear radiation thermometer suffered from increasing deviation of the results with temperature and instability of the calibration [Publ.IV]. The reasons for the deviation are discussed in [Publ.IV]. The linear radiation thermometer was exchanged, and subsequent measurements indicated that the problems related with deviation and instability had disappeared [Publ.IV]. The faulty measurements could not necessarily have been seen in the calibrations with one fixed point cell only. They are revealed, if a high temperature fixed point or VTBB with filter radiometers is used [Publ.IV].

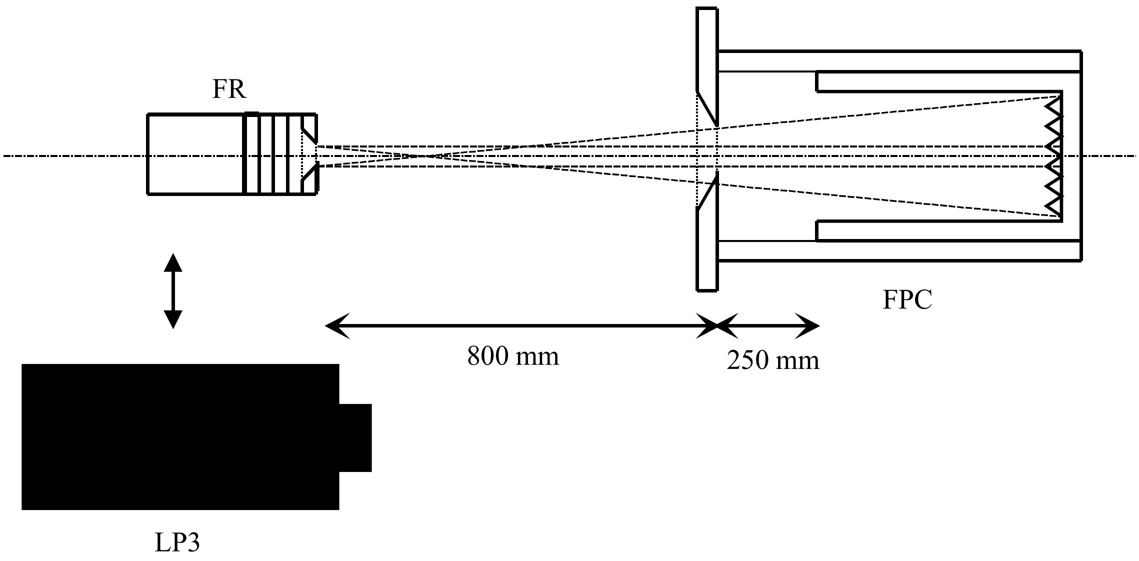

Figure 14. Radiation temperature measurement facility of MIKES.

3.4 Comparisons of the radiation temperature scales

Comparison measurements are commonly carried out to verify accuracies of the radiation temperature and radiance scales of NMIs [112,113,114,115,Publ.V]. The comparisons reported in [112,113,114,115,Publ.V] have been carried out in variable temperature ranges between 1370 K and 3300 K. The comparison measurements of radiation temperature scales are important, because presently there are no fixed points above copper freezing point, 1357.77 K.

A comparison between MIKES and PTB was arranged in March 2007 using the Primary Temperature Radiator (PriTeRa) facility of PTB [116]. The temperature range of the comparison was 1570 K – 2770 K. The measurement equipment is presented in Figure 15. MIKES's measuring equipment consisted of the linear radiation thermometer LP3 and the filter radiometers described in Chapter 3.3. PTB's measuring equipment consisted of a linear radiation thermometer LP3 and a filter radiometer with nominal wavelength of 800 nm. The calibration of the PTB LP3 is described in [115] and the filter radiometer in [117,118]. The measurement artifact was a HTBB of type BB3200pg [17].

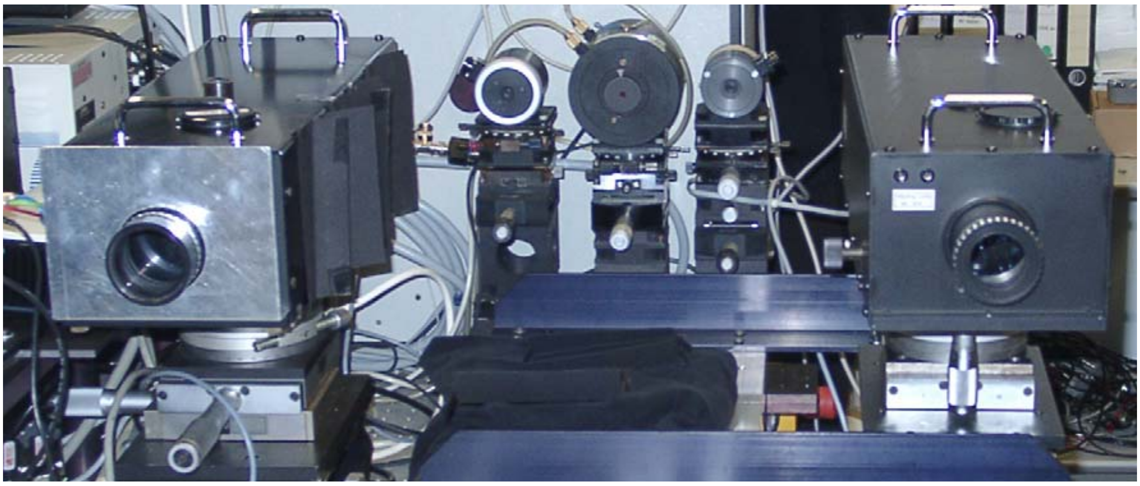

Figure 15. Measurement equipment installed on a translator stage. From left to right: PTB-LP3, MIKES-FR1, PTB-FR, MIKES-FR2 and MIKES-LP3.

The comparison project included comparisons of temperature scales based on both ITS-90 and thermodynamics. The results showed partial agreement. In the ITS-90 comparison carried out using the linear radiation thermometers, the results were in agreement. The agreement can be seen in Figure 16. In the comparison of thermodynamic temperatures, carried out with filter radiometers, two MIKES filter radiometers are in agreement with each other, with PTB's equipment and with the ITS-90 based scale. The other two MIKES filter radiometers deviated from the others. This deviation can be seen in Figure 17.

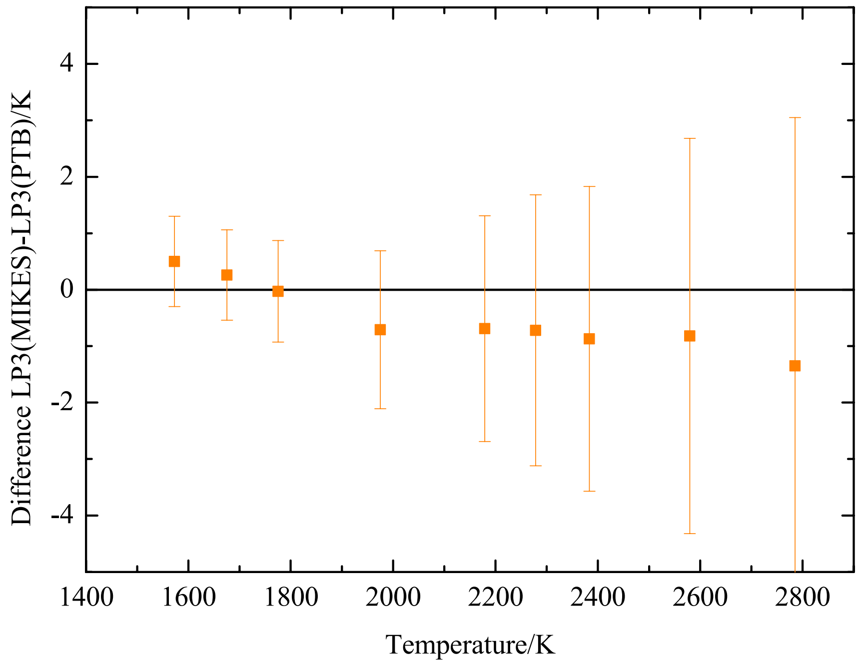

Figure 16. Difference between the measurement results of the LP3-MIKES and LP3-PTB. Both LP3s were calibrated according to ITS-90.

The reasons for the deviation are discussed in [Publ.V]. The measurements with the $V(\lambda)$–filter and the filter radiometer calibrated as a complete package using laser scanning were successful, which indicates that the problems are related with the interchangeable interference filters. One possible reason is the slightly different measurement geometries in the filter transmittance measurements and in the actual temperature measurements. I conclude from our measurements that the geometries should be matched as carefully as possible [119].

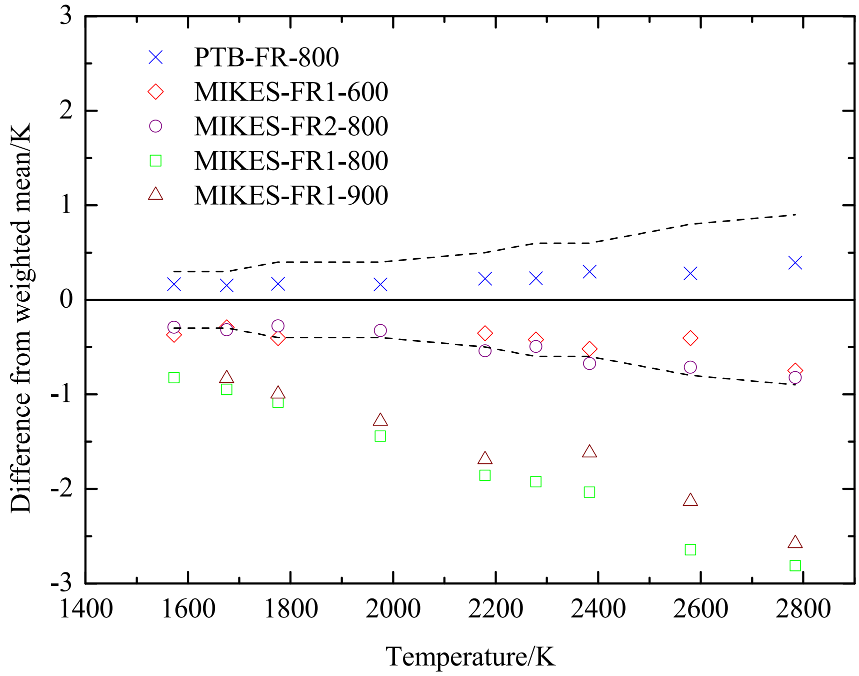

Figure 17. Deviation of the different filter radiometers from the weighted mean. The mean was calculated from the results of PTB-FR-800, MIKES-FR1-600 and MIKES-FR2-800 using the relative weight of 2 for PTB-FR and 1 for both MIKES-FRs. The dashed lines represent the expanded ($k = 2$) uncertainty of MIKES-FR2-800.

4 Conclusions

In this thesis, a physical model for spectral irradiance standard lamps was developed. The model could interpolate and extrapolate the spectral irradiances of FEL and DXW type incandescent lamps in the wavelength range 340 nm – 850 nm from two or three measured spectral irradiance values. The model comprised Planck's radiation law, spectral emissivity of tungsten, a geometrical factor, and a measured spectral residual correction. The residual correction function was determined by measuring the spectra of an FEL lamp at different temperatures. The comparisons with the calibrations of MIKES/TKK and NPL indicate that the model could interpolate and extrapolate the spectral irradiances of the lamps with less than 1 % deviation from the existing calibrations.

The spectral irradiance scales of MIKES/TKK and NMC were compared using NMC's new MWFR facility. The new scale realization showed good agreement with the NMC's existing scale and with the assigned values of the MIKES/TKK's transfer standard. With help of the comparison, the long-term stability of the scales could be studied. The stability was good in visible and near infrared regions. In the UV region, the difference increased up to 2.8 %. The reproducibility was still within expanded uncertainties of the comparison.

The spectral irradiance scale of NIMT was linked to the KCRV using MIKES/TKK as a link. I suggested a new method for uncertainty estimation in the linking process. The method took advantage of the division of the uncertainties to components related to correlated and uncorrelated effects between the measurements. With the new method, the uncertainty due to linking could be estimated more realistically than before. The overall uncertainty due to linking could be reduced, if a linking NMI with small uncertainties related to uncorrelated effects between measurements and good scale reproducibility were selected.

Radiation temperature measurements using filter radiometers were carried out at MIKES. The functionality of the filter radiometers was checked with a Ag fixed point cell. The comparison with an ITS-90 based method showed agreement within uncertainties in the temperature range 1370 K – 1770 K. Filter radiometers provided a good way to assure the quality of extrapolation of the linear radiation thermometers in the temperatures above Cu freezing point.

The radiation temperature scales of MIKES and PTB were compared in the temperature range 1570 K – 2770 K. Both thermodynamic temperatures and the ITS-90 based realizations were compared. The results showed partial agreement: while the ITS-90 scale and two out of four filter radiometers were in good agreement with the PTB's measurement results, two of the filter radiometers deviated from the others.

With help of the improvements presented in this thesis, a simple spectral irradiance scale could be derived from two or three measurement points only. The spectral irradiance of a lamp could also be predicted from the photometric or electrical properties of the lamp. Using the methods presented in this thesis, the quality of the scales can be assured and the uncertainties can be estimated more realistically than before.

5 References

[1] M Planck: Ueber das Gesetz der Energieverteilung im Normalspectrum, *Ann. Phys.* **309**, 553-563 (1901).

[2] H Preston-Thomas: The International Temperature Scale of 1990, *Metrologia* **27**, 3-10 (1990).

[3] K Anhalt, J Hartmann, D Lowe, G Machin, M Sadli and Y Yamada: Thermodynamic temperature determinations of Co-C, Pd-C, Pt-C and Ru-C eutectic fixed-point cells, *Metrologia* **43**, 78-83 (2006).

[4] Y Yamada, B Khlevnoy, Y Wang, T Wang and K Anhalt: Application of metal (carbide)-carbon eutectic fixed points in radiometry, *Metrologia* **43**, 140-144 (2006).

[5] Y Yamada, Y Wang and N Sasajima: Metal carbide-carbon peritectic systems as high-temperature fixed points in thermometry, *Metrologia* **43**, L23-L27 (2006).

[6] Y Yamada, Y Wang, W Zheng and N Sasajima: A study of the Metal Carbide-Carbon Peritectic Phase Transition for the Cr-C system, *Int. J. Thermophys.* **27**, 2028-2040 (2007).

[7] W Zheng, Y Yamada and Y Wang: Investigation of the Cr3C2-C Peritectic Fixed Point, *Int. J. Thermophys.* **28**, 935-943 (2008).

[8] N Sasajima and Y Yamada: Investigation of TiC-C Eutectics and WC-C Peritectics High-Temperature Fixed Points, *Int. J. Thermophys.* **28**, 944-957 (2008).

[9] N P Fox: Primary radiometric quantities and units, *Metrologia* **37**, 501-513 (2000).

[10] P Kärhä, P Toivanen, F Manoochehri and E Ikonen: Development of a detector-based absolute spectral irradiance scale in the 380-900 nm spectral range, *Appl. Opt.* **36**, 8909-8918 (1997).

[11] T Kübarsepp, P Kärhä, F Manoocheri, S Nevas, L Ylianttila and E Ikonen: Spectral irradiance measurements of tungsten lamps with filter radiometers in the spectral range 290 nm to 900 nm, *Metrologia* **37**, 305-312 (2000).

[12] H W Yoon, C E Gibson and P Y Barnes: The realization of the NIST detector-based spectral irradiance scale, *Metrologia* **40**, 172-176 (2003).

[13] H W Yoon, D W Allen, C E Gibson, M Litorja, R D Saunders, S W Brown, G P Eppeldauer and K R Lykke: Thermodynamic-temperature determinations of the Ag and Au freezing temperatures using a detector-based radiation thermometer, *Appl. Opt.* **46**, 2870-2880 (2007).

[14] N P Fox, J E Martin and D H Nettelton: Absolute spectral radiometric determination of the thermodynamic temperatures of the melting/freezing points of gold, silver and aluminium, *Metrologia* **28**, 357-374 (1991).

[15] D R Taubert, J Hartmann, J Hollandt and J Fischer: Investigation of the Accuracy of the ITS-90 with Reference to Thermodynamic Temperature in the Range from 400 °C up to 600 °C, *Temperature: Its Measurement and Control in Science and Industry* **7**, 7-12, ed. D C Ripple, AIP (2003).

[16] N Noulkow, R D Taubert, P Meindl and J Hollandt: Infrared Filter Radiometers for Thermodynamic Temperature Determination below 660 °C, *Int. J. Thermophys.* **30**, 131-143 (2009).
[17] V I Sapritsky, B B Khlevnoy, V B Khromchenko, B E Lisiansky, S N Mekhontsev, U A Melenevsky, S P Morozova, A V Prokhorov, L N Samoilov, V I Shapoval, K A Sudarev and M F Zelener: Precision blackbody sources for radiometric standards, *Appl. Opt.* **36**, 5403-5408 (1997).
[18] V I Sapritsky: Black-body radiometry, *Metrologia* **32**, 411-417 (1995/96).
[19] E G Zubler and F A Mosby: An Iodine Incandescent Lamp with Virtually 100 Per Cent Lumen Maintenance, *Illum. Eng.* **54**, 734-740 (1959).
[20] E R Woolliams, N P Fox, M G Cox, P M Harris and N J Harrison: Final report on CCPR-K1.a: Spectral irradiance from 250 nm to 2500 nm, *Metrologia* **43** (Tech. Suppl.) 02003 (2006).
[21] P Sperfeld: Final report on the CIPM key comparison CCPR-K1.b: Spectral irradiance 200 nm to 350 nm, *Metrologia* **45** (Tech. Suppl.) 02002 (2008).
[22] M Ojanen, M Shpak, R Leecharoen, P Kärhä and E Ikonen: Report on the Spectral Irradiance Comparison EURAMET.PR-K1.a.1 between MIKES (Finland) and NIMT (Thailand), *Metrologia* **46** (Tech. Suppl.) 02001 (2009).
[23] M Stock, J Fischer, R Friedrich, H J Jung, R Thornagel, G Ulm and B Wende: Present State of the Comparison between Radiometric Scales Based on Three Primary Standards, *Metrologia* **30**, 439-449 (1993).
[24] J C de Vos: A new determination of the emissivity of tungsten ribbon, *Physica* **20**, 690-714 (1954).
[25] R M Pon and J P Hessler: Spectral emissivity of tungsten: analytic expressions for the 340-nm to 2.6 μm spectral region, *Appl. Opt*. **23**, 975-976 (1984).
[26] F Wilkinson, G Xu and Y J Liu: Final report on CCPR-K1.a.1: Bilateral comparison of spectral irradiance between NMIA (Australia) and SPRING (Singapore), *Metrologia* **43** (Tech. Suppl.) 02002 (2006).
[27] Mikron Infrared Inc.: *The Theoretical Basis For Radiation Measurements – Blackbody Radiation*, available online at http://www.mikroninfrared.com (24.01.2010).
[28] S Galal Yousef, P Sperfeld and J Metzdorf: Measurement and calculation of the emissivity of a high-temperature black body, *Metrologia* **37**, 365-368 (2000).
[29] A V Prokhorov: Monte Carlo method in optical radiometry, *Metrologia* **35**, 465-471 (1998).
[30] H Preston-Thomas, P Bloembergen and T J Quinn: *Supplementary information for the international temperature scale of 1990*, Bureau International des Poids et Mesures (1990).
[31] P Sperfeld, S Galal Yousef, J Metzdorf, B Nawo and W Möller: The use of self-consistent calibrations to recover absorption bands in the black-body spectrum, *Metrologia* **37**, 373-376 (2000).
[32] P Sperfeld, S Pape, B Khlevnoy and A Burdakin: Performance limitations of carbon-cavity blackbodies due to absorption bands at the highest temperatures, *Metrologia* **46**, S170-S173 (2009).

[33] M White, N P Fox, V E Ralph and N J Harrison: The characterization of a high-temperature black body as the basis for the NPL spectral-irradiance scale, *Metrologia* **32**, 431-434 (1995/96).

[34] P Sperfeld, J Metzdorf, N J Harrison, N P Fox, B B Khlevnoy, V B Khromchenko, S N Mekhontsev, V I Shapoval, M F Zelener and V I Sapritsky: Investigation of high-temperature black body BB3200, *Metrologia* **35**, 419-422 (1998).

[35] E R Woolliams, N J Harrison and N P Fox: Preliminary results of the investigation of a 3500 K black body, *Metrologia* **37**, 501-504 (2000).

[36] P-S Shaw, U Arp, R D Saunders, D-J Shin, H W Yoon, C E Gibson, Z Li, A C Parr and K R Lykke: Synchrotron radiation-based irradiance calibration from 200 to 400 nm at the Synchrotron Ultraviolet Radiation Facility III, *Appl. Opt.* **46**, 25-35 (2007).

[37] U Arp, R Friedman, M L Furst, S Makar and P-S Shaw: SURF III – an improved storage ring for radiometry, *Metrologia* **37**, 357-360 (2000).

[38] R Thornagel, R Klein and G Ulm: The electron storage ring BESSY II as a primary source standard from the visible to the X-ray range, *Metrologia* **38**, 385-389 (2001).

[39] R Klein, G Brandt, R Fliegauf, A Hoehl, R Müller, R Thornagel and G Ulm: The Metrology Light Source operated as a primary source standard, *Metrologia* **46**, S266-S271 (2009).

[40] S I Anevsky, A E Vernyj, V B Khromchenko, V S Panasyuk and V I Sapritsky: Realization of a spectral radiance scale in the 40-250 nm spectral region based on a TROLL-type synchrotron, *Nucl. Instrum. Methods A* **347**, 573-576 (1994).

[41] T Zama and I Saito: Improvement of the beamline for calibration of the transfer standard in the UV and VUV regions, *Metrologia* **40**, S115-S119 (2003).

[42] P J Key: Synchrotron Radiation as a Standard of Spectral Emission, *Metrologia* **6**, 97-103 (1970).

[43] B Wende: Radiometry with synchrotron radiation, *Metrologia* **32**, 419-424 (1995/96).

[44] J Schwinger: On the Classical Radiation of Accelerated Electrons, *Phys. Rev.* **12**, 1912-1925 (1949).

[45] G Ulm: Radiometry with synchrotron radiation, *Metrologia* **40**, S101-S106 (2003).

[46] Cathodeon: *Deuterium lamps*. Cathodeon Ltd, Cambridge.

[47] J Hollandt, U Becker, W Paustian, M Richter and G Ulm: New developments in the radiance calibration of deuterium lamps in the UV and VUV spectral range at the PTB, *Metrologia* **37**, 563-566 (2000).

[48] R P Lambe, R Saunders, C Gibson, J Hollandt and E Tegeler: A CCPR international comparison of spectral radiance measurements in the air-ultraviolet, *Metrologia* **37**, 51-54 (2000).

[49] P Sperfeld, K D Stock, K-H Raatz, B Nawo and J Metzdorf: Characterization and use of deuterium lamps as transfer standards of spectral irradiance, *Metrologia* **40**, S111-S114 (2003).

[50] Spectronic: *Spectronic Analytical Instruments*, available online at http://www.spectronic.co.uk/ (24.01.2010).

[51] J Metzdorf, A Sperling, S Winter, K-H Raatz and W Möller: A new FEL-type quartz-halogen lamp as an improved standard of spectral irradiance, *Metrologia* **35**, 423-426 (1998).

[52] N J Harrison, E R Woolliams and N P Fox: Evaluation of spectral irradiance transfer standards, *Metrologia* **37**, 453-456 (2000).

[53] L Ylianttila, K Jokela and P Kärhä: Ageing of DXW-lamps, *Metrologia* **40**, S120-S123 (2003).

[54] K D Stock, K-H Raatz, P Sperfeld, J Metzdorf, T Kübarsepp, P Kärhä, E Ikonen and L Liedquist: Detector-stabilized FEL lamps as transfer standards in an international comparison of spectral irradiance, *Metrologia* **37**, 441-444 (2000).

[55] R D Larrabee: Spectral Emissivity of Tungsten, *J. Opt. Soc. Am.* **49**, 619-625 (1959).

[56] V D Dmitriev and G K Kholopov: Radiant emissivity of tungsten in the infrared region of the spectrum, *Zhurnal Priklandnoi Spektroskopii* **2**, 481-488 (1965).

[57] V D Dmitriev and G K Kholopov: Radiant emissivity of a tungsten strip in the visible and infrared, *Zhurnal Priklandnoi Spektroskopii* **6**, 425-430 (1967).

[58] F J Studer and R F VanBeers: Modification of Spectrum of Tungsten Filament Quartz-Iodine Lamps due to Iodine Vapor, *J. Opt. Soc. Am.* **54**, 945-947 (1964).

[59] W J Van Den Hoek and E G Berns: Emission lines in the spectra of halogen incandescent lamps, *Light. Res. Technol.* **2**, 143-146 (1975).

[60] L Fu, R Leutz and H Ries: Physical modeling of filament light sources, *J. Appl. Phys.* **100**, 103528 (8 pages) (2006).

[61] L Fu: Increasing the Brightness of Light Sources, *Dissertation zur Erlangung des Doktorgrades der Naturwissenschaften* (Philipps Universität, Marburg, 2006).

[62] J H Walkers, R D Saunders, J K Jackson and D A McSparron: NBS measurement services: Spectral irradiance calibrations, *Natl. Bur. Stand. Spec. Publ.* **250-20**, 25 (1987).

[63] G Andor: New data-reduction method in detector-based spectral irradiance measurements, *Metrologia* **32**, 495-496 (1995/96).

[64] L P Boivin: Calibration of incandescent lamps for spectral irradiance by means of absolute radiometers, *Appl. Opt.* **19**, 2771-2780 (1980).

[65] L K Huang, R P Cebula and E Hilsenrath: New procedure for interpolating NIST FEL lamp irradiances, *Metrologia* **35**, 381-386 (1998).

[66] G Andor: Approximation function of spectral irradiance of standard lamps, *Metrologia* **35**, 427-429 (1998).

[67] R H Knibbs: The measurement of thermal expansion coefficient of tungsten at elevated temperatures, *J. Phys. E: Sci. Instrum.* **2**, 515-517 (1969).

[68] P N V'Yugov and V S Gumenyuk: Thermal expansion of tungsten and tantalum in the range 1500 – 3000 °C, *High Temp.* **3**, 879-880 (1965).

[69] G A W Rutgers and J C de Vos: Relation between brightness temperature, true temperature and colour temperature of tungsten. Luminance of tungsten, *Physica* **20**, 715-720 (1954).

[70] W E Forsythe and E M Watson: Resistance and Radiation of Tungsten as a Function of Temperature, *J. Opt. Soc. Am.* **24**, 114-118 (1934).

[71] G A Zhorov: Electrical resistivity and emissivity of some transition metals and alloys in the high-temperature range, *High Temp*. **10**, 1202-1204 (1972).

[72] B Wilthan, C Cagran and G Pottlacher: Combined DSC and Pulse-Heating Measurements of Electrical Resistivity and Enthalpy of Tungsten, Niobium, and Titanium, *Int. J. Thermophys*. **26**, 1017-1029 (2005).

[73] J E Martin, N P Fox and P J Key: A cryogenic radiometer for Absolute Radiometric Measurements, *Metrologia* **21**, 147-155 (1985).

[74] T R Gentile, J M Houston, J E Hardis, C L Cromer and A C Parr: National Institute of Technology high-accuracy cryogenic radiometer, *Appl. Opt.* **35**, 1056-1068 (1996).

[75] T Varpula, H Seppä and J-M Saari: Optical Power Calibration Based on a Stabilized Green He-Ne Laser and a Cryogenic Absolute Radiometer, *IEEE Trans. Instrum. Meas.* **38**, 558-564 (1989).

[76] L P Boivin and K Gibb: Monochromator-based cryogenic radiometry at the NRC, *Metrologia* **32**, 565-570 (1995/96).

[77] C A Schrama, R Bosma, K Gibb, H Rejn and P Bloembergen: Comparison of monochromator-based and laser-based cryogenic radiometry, *Metrologia* **35**, 431-435 (1998).

[78] P Sperfeld, J Metzdorf, S Galal Yousef, K D Stock and W Möller: Improvement and extension of the black-body-based spectral irradiance scale, *Metrologia* **35**, 267-271 (1998).

[79] A A Gaertner: Spectral irradiance calibrations at the National Research Council of Canada (NRC), *J. Mod. Opt.* **56**, 1488-1496 (2009).

[80] D-J Shin, C-W Park, D-H Lee, S-C Park, Y-W Kim, B-H Kim, S-N Park and B B Khlevnoy: Spectral Irradiance Calibration Facility of KRISS, *Proc. NEWRAD 2008, 10th Int. Conf. on Development and Applications in Novel Radiometry* (Daejeon, South Corea, 2008), 327-328.

[81] C Carreras and A Corrons: Absolute spectroradiometric and photometric scales based on an electrically calibrated pyroelectric radiometer, *Appl. Opt.* **20**, 3530-3534 (1981).

[82] P Corredera, A Corróns, A Pons and J Campos: Absolute spectral irradiance scale in the 700-2400 nm spectral range, *Appl. Opt.* **29**, 3530-3534 (1990).

[83] L P Boivin and A A Gaertner: Realization of a spectral irradiance scale in the near infrared at the National Research Council of Canada, *Appl. Opt.* **31**, 6082-6095 (1992).

[84] M Durak and F Samadov: Realization of a filter radiometer-based irradiance scale with high accuracy in the region from 286 nm to 901 nm, *Metrologia* **41**, 401-406 (2004).

[85] P Kärhä, A Haapalinna, P Toivanen, F Manoochehri and E Ikonen: Filter radiometry based on direct utilization of trap detectors, *Metrologia* **35**, 255-259 (1998).

[86] E W M van der Ham, H C D Bos and C A Schrama: Primary realization of a spectral irradiance employing monochromator-based cryogenic radiometry between 200 nm and 20 μm, *Metrologia* **40**, S177-S180 (2003).
[87] B Hemming, E Ikonen and M Noorma: Measurement of Aperture Diameters using an Optical Coordinate Measuring Machine, *Int. J. Optomechatronics* **1**, 297-311 (2007).
[88] F. Manoochehri and E. Ikonen: High-accuracy spectrometer for measurement of regular spectral transmittance, *Appl. Opt.* **34**, 3686-3692 (1995).
[89] *Organizational structure of the CIPM MRA.* Available online at http://www.bipm.org/en/cipm-mra/organization.html (24.01.2010).
[90] T Kübarsepp, H W Yoon, S Nevas, P Kärhä and E Ikonen: Comparison of spectral irradiance scales between the NIST and the HUT, *Metrologia* **39**, 399-402 (2002).
[91] F Delahaye and T J Witt: Linking the results of key comparison CCEM-K4 with the 10 pF results of EUROMET project 345, *Metrologia* **39** (Tech. Suppl.) 01005 (2002).
[92] C Elster, A Link and W Wöger: Proposal for linking the results of CIPM and RMO key comparisons, *Metrologia* **40**, 189-194 (2003).
[93] J E Decker, A G Steele and R J Douglas: Measurement science and the linking of CIPM and regional key comparisons, *Metrologia* **45**, 223-223 (2008).
[94] E Ikonen, J Hovila and S N Park: Uncertainties in linking bilateral and regional key comparisons to the CCPR key comparison, presented at the *2nd CIE Expert Symposium on Measurement Uncertainty* (Braunschweig, Germany, June 11-17, 2006).
[95] BIPM, IEC, IFCC, ILAC, ISO, IUPAC, IUPAP and OIML: *Evaluation of Measurement Data – Guide to the Expression of Uncertainty in Measurement*, JCGM 100:2008 (GUM 1995 with minor corrections, 2008).
[96] T J Quinn: News from the BIPM, *Metrologia* **38**, 89-94 (2001).
[97] J Hartmann and L Werner: Radiation Thermometry Toward the Triple Point of Water?, *Int. J. Thermophys.* **29**, 1052-1065 (2008).
[98] D R White and P Saunders: The propagation of uncertainty on interpolated scales, with examples from thermometry, *Metrologia* **37**, 285-293 (2000).
[99] P Saunders and D R White: Interpolation errors for radiation thermometry, *Metrologia* **41**, 41-46 (2004).
[100] P Saunders and D R White: Propagation of Uncertainty Due to Non-linearity on Radiation Thermometers, *Int. J. Thermophys.* **28**, 2098-2110 (2007).
[101] J Fischer, M Battuello, M Sadli, M Ballico, S N Park, P Saunders, Y Zundong, B C Johnson, E van der Ham, F Sakuma, G Machin, N Fox, W Li, S Ugur and M Matveyev: Uncertainty Budgets for Realization of ITS-90 by Radiation Thermometry, *Temperature: Its Measurement and Control in Science and Industry* **7**, 631-638, ed. D C Ripple, AIP (2003).
[102] G Machin, P Bloembergen, J Hartmann, M Sadli and Y Yamada: A Concentred International Project to Establish High-Temperature Fixed Points for Primary Thermometry, *Int. J. Thermophys.* **28**, 1976-1982 (2007).
[103] T J Quinn: News from the BIPM, *Metrologia* **34**, 187-194 (1997).

[104] Y Yamada, H Sakate, F Sakuma and A Ono: Radiometric observation of melting and freezing plateaus for a series of metal-carbon eutectic points in the range 1330 °C to 1950 °C, *Metrologia* **36**, 207-209 (1999).

[105] K Anhalt, J Hartmann, D Lowe, G Machin, M Sadli, Y Yamada and P Bloembergen: A comparison of Co-C, Pd-C, Pt-C, Ru-C and Re-C eutectic fixed points independently manufactured by three different institutes, *Proc. NEWRAD 2005, 9th Int. Conf. on Development and Applications in Novel Radiometry* (WRC/PMOD, Davos, Switzerland, 2005), Ed. J Gröbner, 289-290.

[106] D Lowe and Y Yamada: Reproducible metal-carbon eutectic fixed points, *Metrologia* **43**, S135-S139 (2006).

[107] J Fischer, G Neuer, E Schreiber and R Thomas: Metrological Characterisation of a new Transfer Standard Radiation Thermometer, *Proc. TEMPMEKO 2001, 8th Int. Symp. on Temperature and Thermal Measurements in Industry and Science* (Berlin, Germany, 2001) Eds. B Fellmuth, J Seidel and G Scholz, 801-806.

[108] P Kärhä, N J Harrison, S Nevas, W S Hartree and I Abu-Kassem: Intercomparison of characterization techniques of filter radiometers in the ultraviolet region, *Metrologia* **40**, S50-S54 (2003).

[109] M Noorma, P Toivanen, F Manoocheri and E Ikonen: Characterization of filter radiometers with wavelength tunable laser source, *Metrologia* **40**, 220-223 (2003).

[110] M Noorma, P Kärhä, T Jankowski, F Manoocheri, T Weckström, L Uusipaikka and E Ikonen: Absolute detector-based radiometric temperature scale, *Proc. TEMPMEKO 2004, 9th Int. Symp. on Temperature and Thermal Measurements in Industry and Science* (FSB/LPM, Zagreb, Croatia, 2004) Eds. D Zvizdic, L G Bermanec, T Veliki and T Stašic, 101-106.

[111] M Noorma: Development of detectors and calibration methods for spectral irradiance and radiometric temperature measurements, *Thesis for degree of Doctor of Technology* (Helsinki University of Technology, Metrology Research Institute, Espoo, Finland 2005).

[112] B B Khlevnoy, N J Harrison, L J Rogers, D F Pollard, N P Fox, P Sperfeld, J Fischer, R Friedrich, J Metzdorf, J Seidel, M L Samoylov, R I Stolyarevskaya, V B Khromchenko, S A Ogarev and V I Sapritsky: Intercomparison of radiation temperature measurements over the temperature range from 1600 K to 3300 K, *Metrologia* **40**, S39-S44 (2003).

[113] F Sakuma, L Ma and J Hartmann: Intercomparison of radiation temperature scales between PTB and NMIJ from 1100°C to 2500 °C, *Proc. SICE2002, 41th SICE Ann. Conf.* (Osaka, Japan, 2002), 58-62.

[114] N J Harrison, N P Fox, P Sperfeld, J Metzdorf, B B Khlevnoy, R I Stolyarevskaya, V B Khromchenko, S N Mekhontsev, V I Shapoval, M F Zelener and V I Sapritsky: International comparison of radiation-temperature measurements with filtered detectors over the temperature range 1380 K to 3100 K, *Metrologia* **35**, 283-288 (1998).

[115] K Anhalt, J Hartmann, J Hollandt, G Machin, D Lowe, H McEvoy, F Sakuma and L Ma, Comparison of high temperature scales of the NMIJ and the NPL with the scale of the PTB from 1300 K to 3200 K, Proc. TEMPMEKO 2004, *9th*

Int. Symp. on Temperature and Thermal Measurements in Industry and Science (FSB/LPM, Zagreb, Croatia, 2004) Eds. D Zvizdic, L G Bermanec, T Veliki and T Stašic, 1063-1068.
[116] J Hartmann, K Anhalt, B Gutschwager, C Monte, P Sperfeld, D Taubert and J Hollandt: The PriTeRa facility of PTB for spectral radiance and irradiance calibrations and radiation thermometry in the range from -170 °C up to 3200 °C and from 200 nm up to 50 µm, *Proc. NEWRAD 2008, 10th Int. Conf. on New Developments and Applications in Optical Radiometry* (Daejeon, Korea, October 13-16, 2008), 231-232.
[117] R Friedrich, J Fischer and M Stock: Accurate calibration of filter radiometers against a cryogenic radiometer using a trap detector, *Metrologia* **32**, 509-513 (1995/96).
[118] D R Taubert, R Friedrich, J Hartmann and J Hollandt: Improved calibration of the spectral responsivity of interference filter radiometers in the visible and near infrared spectral range at PTB, *Metrologia* **40**, S35-S38 (2003).
[119] A A Gaertner and L P Boivin: Some problems in realizing an infrared spectral-irradiance scale from 1500 nm to 2400 nm at the NRC, *Metrologia* **32**, 615-619 (1995/96).

ISBN 978-952-60-3155-2
ISBN 978-952-60-3156-9 (PDF)
ISSN 1795-2239
ISSN 1795-4584 (PDF)